QUARTERLY OF APPLIED MATHEMATICS

VOLUME LIX JUNE · 2001 NUMBER 2

JUNE 2001, PAGES 193–223

LOAD MAXIMUM BEHAVIOR IN THE INFLATION OF HOLLOW SPHERES OF INCOMPRESSIBLE MATERIAL WITH STRAIN-DEPENDENT DAMAGE

BY

H. E. HUNTLEY (*Department of Mechanical Engineering, University of Michigan-Dearborn, Dearborn, MI*),

A. S. WINEMAN (*Department of Mechanical Engineering, University of Michigan, Ann Arbor, MI*),

AND

K. R. RAJAGOPAL (*Department of Mechanical Engineering, Texas A & M University, College Station, TX*)

Abstract. Carroll has shown three qualitatively different cases of behavior in the load-expansion relation for the inflation of hollow incompressible isotropic elastic spheres. Each of these cases was related to material response in uniaxial compression (or equal biaxial extension). For "type A" materials, load increases monotonically with expansion; for "type B" materials, load increases monotonically and then decreases; for "type C" materials, load increases monotonically, decreases, and again increases. The present work discusses the monotonicity properties of the load-expansion relation when rubbery materials undergo microstructural change or damage. The analysis is carried out using a constitutive equation for materials undergoing continuous scission and reformation of macromolecular junctions. Results are presented for the case when this leads to softening of response. For "type A", sufficient softening can cause loss of monotonicity; for "type B", the softening leads to loss of monotonicity at smaller levels of inflation and lower loads.

1. Introduction. The general form of the constitutive equation for nonlinear elastic solids is based on assumptions which imply that stress arises from a single unchanging material micromechanism at all stages of deformation. Rajagopal and Wineman [1992] have recently presented a constitutive theory which can be used to model the mechanical response of rubber-like materials that exhibit changes in micromechanism. In their model, the stress is determined by one micromechanism within some regime of deformation; as deformation increases, a new micromechanism arises which affects the mechanical

Received November 9, 1995.
2000 *Mathematics Subject Classification.* Primary 74B20.

response. They considered the particular example in which the material acts as a rubbery solid if the deformations are relatively small. When deformations become sufficiently large, network junctions in the original material break and then reform to produce a new network with a new unstressed local configuration. Their work allowed for continuous conversion of the original material to new networks as deformation proceeds. It was shown that the material can undergo substantial softening and that there is permanent set when the applied load is removed. It is emphasized that the term "network" is used in this paper for convenience in presenting modeling concepts. It is used broadly to denote a material's microstructure; it is not intended to imply any specific microstructural process.

There have been several applications of this constitutive theory to problems involving nonhomogeneous deformations. The examples all assume that the material is incompressible and that new networks are generated at sufficiently large deformations. Wineman and Rajagopal [1990] studied the finite extension and torsion of a circular cylinder. Huntley [1992] considered the circumferential shear of a hollow concentric cylinder whose inner surface is fixed and whose outer surface is rotated about the centerline. Huntley [1992] also analyzed the radial expansion of thick-walled hollow spheres under either internal pressure or external radial tension. Wineman and Huntley [1994] studied a circular rubber membrane that is fixed at its boundary and subjected to a uniform pressure over one of its surfaces. In each of these studies, when the deformation is sufficiently large, there is a region of original material separated from a region of multi-network material by an interface whose location varies with the size of the deformation.

The constitutive theory not only has an important influence on the local material behavior, but also affects the global load-expansion response. The present work considers a specific case of the latter for the problem of the radial expansion of a thick-walled hollow sphere. Of particular interest is the relation between the current inner radius and either the internal pressure or the external radial tension. Carroll [1987] presented a thorough discussion of the load-expansion relation for incompressible isotropic nonlinear elastic materials. He provided general results that relate the loss of monotonicity in the load-expansion response of a material to the properties of its equal biaxial plane stress-stretch relationship. In the present work, Carroll's analysis is modified so as to account for the influence of microstructural change on the loss of monotonicity in the load-expansion relation.

The constitutive equation is presented in Sec. 2 and the equations governing the radial expansion of a hollow thick-walled sphere are presented in Sec. 3. Section 4 contains a discussion of the conditions for monotonicity of response of the load-expansion relation. First, Carroll's analysis for elastic materials is reviewed. It is then extended to account for elastic materials undergoing microstructural change. The numerical method of solution is outlined in Sec. 5. Results for numerical examples are discussed in Sec. 6. Conclusions are presented in Sec. 7.

2. Constitutive equation. Consider a sample of material undergoing a homogeneous deformation described by $\mathbf{x} = \mathbf{x}(\mathbf{X}, t)$, where $\mathbf{x}$ is the current position of a particle located at $\mathbf{X}$ in the undeformed reference configuration, when $t = 0$. The deformation gradient associated with this mapping is $\mathbf{F} = \partial\mathbf{x}/\partial\mathbf{X}$ and the left Cauchy-Green tensor

is given by $\mathbf{B} = \mathbf{F}\mathbf{F}^{\mathrm{T}}$. Assume that there is a range of deformation on which the material behaves as an isotropic, incompressible, nonlinear Green elastic solid. It is well known (e.g., Spencer [1980]) that the Cauchy stress $\mathbf{T}$ for this material takes the form

$$\mathbf{T} = -p\mathbf{I} + 2[W_1^{(1)}\mathbf{B} - W_2^{(1)}\mathbf{B}^{-1}], \tag{1}$$

where $-p\mathbf{I}$ is an indeterminate hydrostatic stress state. It will be convenient to denote the extra stress by $\mathcal{T} = \mathbf{T} + p\mathbf{I}$. $W^{(1)} = W^{(1)}(I_1, I_2)$ is the strain energy per unit volume, where $I_1 = \mathrm{tr}(\mathbf{B})$ and $I_2 = \mathrm{tr}(\mathbf{B}^{-1})$ are the first two invariants of $\mathbf{B}$. Also, $W_1^{(1)} = \partial W^{(1)}/\partial I_1$ and $W_2^{(1)} = \partial W^{(1)}/\partial I_2$.

An activation criterion determines when the original material network begins to undergo microstructural change and form new networks. This criterion is taken to be expressed as a function of the deformation gradient $\mathbf{F}$ which vanishes when microstructural change begins. Material frame indifference, isotropy and incompressibility imply that the activation criterion can be expressed in terms of the invariants of $\mathbf{B}$: $A(I_1, I_2) = 0$.

Transformation of the original microstructural network is assumed to be continuous with increasing deformation. Introduce a scalar deformation state parameter s whose value is determined by the extent of deformation. It can be expressed in terms of the stretch invariants: $s = s(I_1, I_2)$. The value of s increases as deformation increases. No unique definition of the term "increasing deformation" is proposed. Instead, as in the previous applications of this constitutive equation (Wineman and Rajagopal [1990]; Huntley [1992]; Wineman and Huntley [1994]), an appropriate form of s is selected for the deformation process under consideration. Recasting the activation criterion in terms of the state parameter gives $A(I_1, I_2) = s(I_1, I_2) - s_a$. Microstructural conversion is initiated when the state parameter s first reaches the conversion-activation value s_a.

For $s < s_a$, no conversion has yet occurred; thus all material is original and the total stress is given by (1). At the current deformation state s, with $s \geq s_a$, stress in the remaining original material is also a function of the current deformation gradient $\mathbf{F}$.

Introduce the scalar-valued conversion rate function $a(s)$. As increasing deformation causes the state parameter to increase beyond $s = s_a$, the conversion rate function determines the amount of network transformation induced by additional deformation. The conversion rate function may have any form respecting the constraints $a(s) = 0$, $s < s_a$ and $a(s) \geq 0$, $s \geq s_a$. $a(s)$ must remain nonnegative in order that an increase in deformation always be associated with additional microstructural change. It is assumed that a is a continuous function of s.

Consider a value of the deformation state parameter $\hat{s} \geq s_a$. It is assumed that a network is formed at this value of the deformation state parameter. Its reference configuration is the configuration of the original material at state $\hat{s}$. It is assumed to be an unstressed configuration for the newly formed network. Stress in such a material network is a function of the subsequent deformation of the network relative to this unstressed configuration. Define the deformation gradient for the material formed at state $\hat{s}$ as $\widehat{\mathbf{F}} = \partial\mathbf{x}/\partial\hat{\mathbf{x}}$, where $\hat{\mathbf{x}}$ is the position of the particle in the configuration corresponding to deformation state $\hat{s}$. Referred to as the relative deformation gradient, $\widehat{\mathbf{F}}$ compares the neighborhood of a particle in the configuration at state s with the configuration of the

new network when it was formed at state $\hat{s}$. The associated relative left Cauchy-Green tensor is given by $\widehat{\mathbf{B}} = \widehat{\mathbf{F}}\widehat{\mathbf{F}}^{\mathrm{T}}$.

Let it be assumed that the material network formed at state $\hat{s}$ is elastic, isotropic, and incompressible. The extra Cauchy stress at state s in a network formed at deformation state $\hat{s}$ then becomes

$$\mathcal{T}^{(2)} = 2[W_1^{(2)}\widehat{\mathbf{B}} - W_2^{(2)}\widehat{\mathbf{B}}^{-1}]. \tag{2}$$

Here $W^{(2)} = W^{(2)}(\hat{I}_1, \hat{I}_2)$ is the strain energy density of the material formed at state $\hat{s}$ and subsequently deformed to state s. $\hat{I}_1$ and $\hat{I}_2$ are the appropriate invariants of $\widehat{\mathbf{B}}$. The strain energy density functions $W^{(1)}$ and $W^{(2)}$ may be of any form. It is assumed that the single function $W^{(2)}$ governs the strain energy density in each newly formed network. The material defined by (2) is not a simple material in the sense of Noll (see Rajagopal [1995]).

Total current stress in the material is taken as the superposition of the contribution from the remaining material of the original network and the contributions from all networks formed at deformation states $\hat{s} \in [s_a, s]$. During a process of increasing deformation the total current stress is given by

$$\mathbf{T} = -p\mathbf{I} + b(s)\mathcal{T}^{(1)} + \int_{s_a}^{s} a(\hat{s})\mathcal{T}^{(2)}d\hat{s}. \tag{3}$$

The function $b(s)$ is the volume fraction of the original network material remaining at state s, with $b(s) = 1$, $s \leq s_a$, and $b(s) \in [0, 1]$, $s \geq s_a$. The volume fraction $b(s)$ decreases as s increases. $\mathcal{T}^{(1)}$, found from (1), is the current stress in the remaining original material. The quantity $a(\hat{s})d\hat{s}$ may be interpreted as the volume fraction of material that ruptures and reforms as the deformation state increases from $\hat{s}$ to $\hat{s} + d\hat{s}$. $\mathcal{T}^{(2)}$, given by (2), is the stress in that portion of newly formed material. With (1) and (2), (3) can be written in the form

$$\mathbf{T} = -p\mathbf{I} + 2b(s)[W_1^{(1)}\mathbf{B} - W_2^{(1)}\mathbf{B}^{-1}] + 2\int_{s_a}^{s} a(\hat{s})[W_1^{(2)}\widehat{\mathbf{B}} - W_2^{(2)}\widehat{\mathbf{B}}^{-1}]d\hat{s}. \tag{4}$$

Equations (3) and (4) are constitutive equations for incompressible materials and respect the requirements of frame indifference and isotropy.

Much of the notation to be used in this article has already been introduced. However, before proceeding to study the application of the constitutive equation, it is important that the notational scheme and the functional dependences that it implies be clearly understood. An overview of the principal elements of the notational system is presented here.

Unhatted kinematic quantities, such as $\mathbf{F}, \mathbf{B}, I_1$, and I_2, are referred to as "current" and compare configuration at the current deformation state s with the initial reference configuration. Kinematic quantities bearing the hat notation ($\widehat{\ }$), such as $\widehat{\mathbf{F}}, \widehat{\mathbf{B}}, \hat{I}_1$, and $\hat{I}_2$, are called "relative" quantities. They represent comparison of the configuration at the current state s with the configuration at state $\hat{s}$.

The superscript $(\ )^{(1)}$ appearing in stress quantities such as $\mathcal{T}^{(1)}$ indicates that the stress is in material of the original microstructural network. Such stresses are functions of the current left Cauchy-Green tensor $\mathbf{B}$. The superscript $(\ )^{(2)}$ appearing, for example, in

$\mathcal{T}^{(2)}$ indicates stress in a material network formed at deformation state $\hat{s}$. These stresses are functions of the relative left Cauchy-Green tensor $\widehat{\mathbf{B}}$. Unsuperscripted stresses, such as $\mathbf{T}$, are total stresses following the superposition given by (3) of stresses in original and newly formed networks. They are thus functions of the current tensor $\mathbf{B}$ and of the relative tensors $\widehat{\mathbf{B}}$ relating the current configuration to each state $\hat{s} \in [s_a, s]$ for increasing deformation. For a process of increasing deformation, unsuperscripted stresses also depend explicitly on the current value of the deformation state parameter s, which appears as the upper limit of integration and as the argument of $b(s)$.

The function $W^{(1)}$ denotes the Helmholtz strain energy density in material of the original network; it is a function of the current stretch invariants I_1 and I_2. $W^{(2)}$ is the strain energy density in the material of a subsequently formed network and is a function of the relative invariants $\hat{I}_1$ and $\hat{I}_2$.

Non-dimensionalized quantities bear the tilde notation ($\tilde{}$), as $\widetilde{\mathbf{T}}$.

For purposes of notational simplicity, none of the functional dependences mentioned above is indicated explicitly when kinematic or stress quantities are written.

3. Formulation.

3.1. *Kinematics of deformation.* Consider a sphere of initial outer radius R_o containing a central spherical cavity of radius R_i. In spherical coordinates, the undeformed sphere occupies the domain

$$D = \{(R, \Phi, \Theta) \colon R \in [R_i, R_o]; \Phi \in [0, \pi]; \Theta \in [0, 2\pi)\}. \tag{5}$$

No restriction is placed on the thickness of the sphere: all values of R_i and R_o, with $R_o > R_i$, are admissible. The sphere is considered to be composed of material that is initially homogeneous, incompressible, elastic, and isotropic.

Let T_o be a radial force per unit current surface area. A uniform radial tensile traction of magnitude T_o is applied at the outer surface. The surface of the inner cavity is traction-free. The resulting deformation is assumed to be spherically symmetric. With (r, ϕ, θ) denoting the current coordinates of the particle initially located at (R, Φ, Θ), the mapping has the form

$$\begin{aligned} r &= r(R), \\ \phi &= \Phi, \\ \theta &= \Theta. \end{aligned} \tag{6}$$

The radial deformation function $r(R)$ is to be found. For the mapping (6) the general deformation gradient in spherical coordinates (e.g., Spencer [1980]) is found to simplify to

$$\mathbf{F} = \mathbf{F}(R) = \operatorname{diag}\left(\frac{dr}{dR}, \frac{r}{R}, \frac{r}{R}\right). \tag{7}$$

The statement of incompressibility, $\det(\mathbf{F}) = 1$, may be written from (7) as

$$\left(\frac{r}{R}\right)^2 \frac{dr}{dR} = 1. \tag{8}$$

Introduce the notation $\lambda = r/R$. The incompressibility condition (8) becomes

$$\lambda^2 \frac{dr}{dR} = 1, \tag{9}$$

which gives $dr/dR = 1/\lambda^2$. Thus the current deformation gradient (7) with respect to the initial coordinates may be written as

$$\mathbf{F} = \operatorname{diag}\left(\frac{1}{\lambda^2}, \lambda, \lambda\right). \tag{10}$$

It can be seen from the deformation gradient (10) that each particle R of the sphere may be regarded as undergoing locally homogeneous equal biaxial extension. The r-, ϕ- and θ-directions are the principal directions of stretch. There is no variation in deformation with the ϕ- and θ-coordinates; the state of equal biaxial extension is a function of the radial coordinate R.

The current left Cauchy-Green tensor and its inverse are found from (10) to be

$$\mathbf{B} = \mathbf{F}\mathbf{F}^{\mathrm{T}} = \operatorname{diag}\left(\frac{1}{\lambda^4}, \lambda^2, \lambda^2\right) \tag{11}$$

and

$$\mathbf{B}^{-1} = \operatorname{diag}\left(\lambda^4, \frac{1}{\lambda^2}, \frac{1}{\lambda^2}\right). \tag{12}$$

The invariants of $\mathbf{B}$ are given by

$$I_1 = 2\lambda^2 + \frac{1}{\lambda^4}; \qquad I_2 = \frac{2}{\lambda^2} + \lambda^4. \tag{13}$$

Note that (8) can be integrated to give the relation

$$\lambda = \lambda(R) = \left[1 + (\lambda_i^3 - 1)\left(\frac{R_i}{R}\right)^3\right]^{1/3}, \tag{14}$$

where λ_i denotes the equal biaxial stretch ratio $\lambda(R_i)$ at the inner surface of the sphere. Once the value of λ_i is specified, (14) gives the stretch ratio distribution $\lambda(R)$ for the entire sphere. λ_i is thus considered a global deformation control parameter in the remainder of this article. It can be seen from (14) that, for a fixed particle label R, λ increases monotonically with λ_i. A process of increasing λ_i thus assures a process of increasing λ for all $R \in [R_i, R_o]$.

Recall the requirement that the deformation state parameter $s(I_1, I_2)$ increase with some measure of the stretch invariants. For $\lambda > 1$, both I_1 and I_2 as given by (13) increase monotonically in λ. Thus s can be expressed as $s(\lambda)$, a monotonically increasing function of λ. The parameter s also increases monotonically with λ_i at fixed R. Equation (14) also reveals that, for a fixed stretch λ_i, λ and hence s decrease monotonically as R increases.

Consider now the material of a particle R that undergoes conversion at some value of the deformation state parameter $\hat{s} \geq s_a$. let $\hat{\lambda}$ be the equal biaxial stretch ratio corresponding to deformation state $\hat{s}$. It follows from (10) that

$$\frac{\partial \hat{\mathbf{x}}}{\partial \mathbf{X}} = \operatorname{diag}\left(\frac{1}{\hat{\lambda}^2}, \hat{\lambda}, \hat{\lambda}\right). \tag{15}$$

Deformation then increases beyond state $\hat{s}$. Note that

$$\widehat{\mathbf{F}} = \mathbf{F}\left(\frac{\partial \hat{\mathbf{x}}}{\partial \mathbf{X}}\right)^{-1} \tag{16}$$

implies that the relative deformation gradient is

$$\widehat{\mathbf{F}} = \operatorname{diag}\left[\left(\frac{\hat{\lambda}}{\lambda}\right)^2, \frac{\lambda}{\hat{\lambda}}, \frac{\lambda}{\hat{\lambda}}\right]. \tag{17}$$

The relative left Cauchy-Green tensor and its inverse are formed from (17) as

$$\widehat{\mathbf{B}} = \widehat{\mathbf{F}}\widehat{\mathbf{F}}^{\mathrm{T}} = \operatorname{diag}\left[\left(\frac{\hat{\lambda}}{\lambda}\right)^4, \left(\frac{\lambda}{\hat{\lambda}}\right)^2, \left(\frac{\lambda}{\hat{\lambda}}\right)^2\right] \tag{18}$$

and

$$\widehat{\mathbf{B}}^{-1} = \operatorname{diag}\left[\left(\frac{\lambda}{\hat{\lambda}}\right)^4, \left(\frac{\hat{\lambda}}{\lambda}\right)^2, \left(\frac{\hat{\lambda}}{\lambda}\right)^2\right]. \tag{19}$$

The relative invariants are found from (18) to be

$$\hat{I}_1 = 2\left(\frac{\lambda}{\hat{\lambda}}\right)^2 + \left(\frac{\hat{\lambda}}{\lambda}\right)^4; \qquad \hat{I}_2 = 2\left(\frac{\hat{\lambda}}{\lambda}\right)^2 + \left(\frac{\lambda}{\hat{\lambda}}\right)^4. \tag{20}$$

3.2. *Stress-stretch relations.* Consider a process in which λ_i increases monotonically. As discussed above, the stretch ratio λ and hence the deformation state parameter s increase monotonically for all $R \in [R_i, R_o]$.

For any particle R that has not undergone microstructural transformation, where $s < s_a$, the nonzero current Cauchy stresses are given by (1), (11), and (12) as

$$\begin{aligned} T_{rr} &= -p + 2\left[\frac{W_1^{(1)}}{\lambda^4} - W_2^{(1)}\lambda^4\right], \\ T_{\theta\theta} &= -p + 2\left[W_1^{(1)}\lambda^2 - \frac{W_2^{(1)}}{\lambda^2}\right], \end{aligned} \tag{21}$$

with p an indeterminate scalar. Also, $T_{\phi\phi} = T_{\theta\theta}$. Note that, since the stretch tensors are diagonal, all shear stress components are identically zero. From (21) it is clear that the extra stress components are functions of λ. As discussed above, however, $\lambda(R)$ is given by (14) at any level of deformation of the sphere, once the deformation control parameter λ_i is prescribed. Thus the extra stresses may also be considered functions of the reference coordinate R.

The normal stress difference, $\overline{T} = \overline{T}(R) = T_{\theta\theta}(R) - T_{rr}(R)$, is of primary interest. From (21), the normal stress difference when $s < s_a$ is seen to be

$$\overline{T} = \overline{T}^{(1)} = 2E^{(1)}\left(\lambda^2 - \frac{1}{\lambda^4}\right), \tag{22}$$

where $E^{(1)}$ is the deformation-dependent modulus of the original material given by

$$E^{(1)} = E^{(1)}(\lambda(R)) = W_1^{(1)} + \lambda^2 W_2^{(1)}. \tag{23}$$

As λ_i increases, particles at some R may stretch to such an extent that $s(\lambda(R)) \geq s_a$. For particles with $s \geq s_a$, the nonzero current Cauchy stresses are formed from (4), (11), (12), (18), and (19) as

$$T_{rr} = -p + 2b(s)\left[W_1^{(1)}\frac{1}{\lambda^4} - W_2^{(1)}\lambda^4\right] + 2\int_{s_a}^{s} a(\hat{s})\left[W_1^{(2)}\left(\frac{\hat{\lambda}}{\lambda}\right)^4 - W_2^{(2)}\left(\frac{\lambda}{\hat{\lambda}}\right)^4\right] d\hat{s},$$

$$T_{\theta\theta} = -p + 2b(s)\left[W_1^{(1)}\lambda^2 - W_2^{(1)}\frac{1}{\lambda^2}\right] + 2\int_{s_a}^{s} a(\hat{s})\left[W_1^{(2)}\left(\frac{\lambda}{\hat{\lambda}}\right)^2 - W_2^{(2)}\left(\frac{\hat{\lambda}}{\lambda}\right)^2\right] d\hat{s}. \tag{24}$$

Again, $T_{\phi\phi} = T_{\theta\theta}$. The normal stress difference for $s \geq s_a$ is found from (24) to be

$$\overline{T} = 2\left\{b(s)E^{(1)}\left(\lambda^2 - \frac{1}{\lambda^4}\right) + \int_{s_a}^{s} a(\hat{s})E^{(2)}\left[\left(\frac{\lambda}{\hat{\lambda}}\right)^2 - \left(\frac{\hat{\lambda}}{\lambda}\right)^4\right] d\hat{s}\right\}, \tag{25}$$

with the deformation-dependent modulus of the newly formed material given by

$$E^{(2)} = E^{(2)}\left(\frac{\lambda}{\hat{\lambda}}\right) = W_1^{(2)} + \left(\frac{\lambda}{\hat{\lambda}}\right)^2 W_2^{(2)}. \tag{26}$$

Since $s = s(\lambda)$ and $\lambda = \lambda(R)$ by (14), each value of λ_i determines a variation of s with R. The state parameter s decreases monotonically with R for all λ_i. Figure 1 shows the general form of the s-R distribution for the sphere at several levels of deformation λ_i. At a low value of $\lambda_i = \lambda_{sm}, s < s_a$ for all $R \in [R_i, R_o]$, as seen in Fig. 1. No microstructural change has occurred; the entire sphere is composed of the original material. Due to the one-to-one correspondence between s and λ, there exists a specific value of λ_i denoted by $\lambda_i = \lambda_a$, with $\lambda_a > \lambda_{sm}$, which corresponds to $s(\lambda_i) = s_a$. Conversion is just initiated at $R = R_i$; $s < s_a$ for all $R \in (R_i, R_o]$. When $\lambda_i = \lambda_{lg}$, where $\lambda_{lg} > \lambda_a$, there is an activation radius R_a defined by $s(\lambda(R_a)) = s_a$, where $\lambda(R_a) = \lambda_a$. $s > s_a$ for $R \in [R_i, R_a)$, while $s < s_a$ for $R \in (R_a, R_o]$. Thus there is an inner spherical region where conversion is taking place and both original material and newly formed networks are present and an outer spherical region composed purely of original material.

The activation value of the stretch ratio λ_a and the activation radius R_a are related by (14). With the substitutions $\lambda = \lambda_a$ and $R = R_a$, (14) can be rearranged to give

$$R_a = R_i\left(\frac{\lambda_i^3 - 1}{\lambda_a^3 - 1}\right)^{1/3}. \tag{27}$$

When λ_a is specified, it is clear from (27) that R_a moves outward as λ_i increases during a process of increasing deformation.

The Cauchy stresses for the inner region undergoing microstructural change, $R \in [R_i, R_a]$, are given by (24). Stresses in the outer region of original material, $R \in [R_a, R_o]$, are given by (21). Note that $R = R_a$ belongs to both of the two closed intervals on R. This holds because the results given by the two stress models (21) and (24) are identical at $R = R_a$.

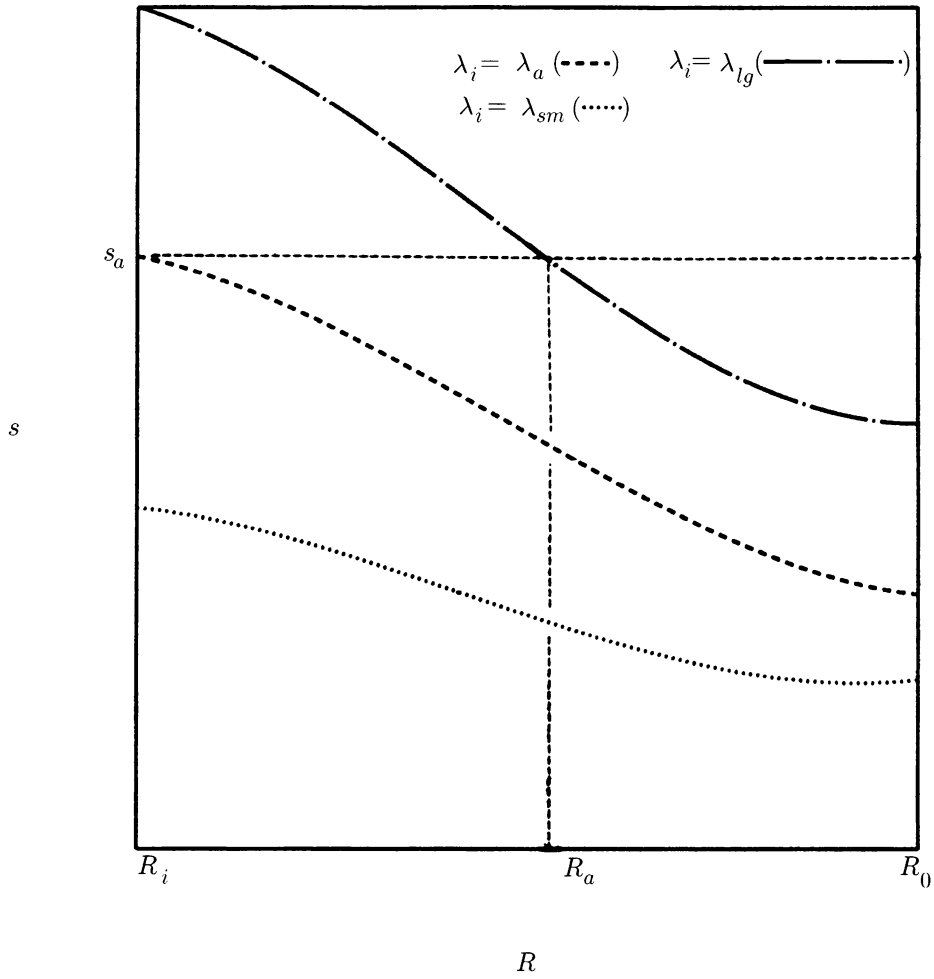

FIG. 1. Typical forms of deformation state parameter vs. radius for various inner surface stretch ratios; activation radius is indicated for $\lambda_i = \lambda_{lg}$.

3.3. *Equilibrium.* It should be noted that the spherical deformation described by (6) is a controllable deformation (Carroll [1967]). For any incompressible isotropic solid, a scalar field p can be found that satisfies the equilibrium equations. Furthermore, it can be shown that $p = p(r)$.

It has been shown that the shear components of the Cauchy stress are identically zero and that the extra stresses $\mathcal{T}_{rr}$ and $\mathcal{T}_{\phi\phi} = \mathcal{T}_{\theta\theta}$ are independent of the coordinates ϕ and θ. When body forces are neglected, and use is made of $T_{\phi\phi} = T_{\theta\theta}$, the equilibrium equations in spherical coordinates (e.g., Spencer [1980]) are reduced to

$$\frac{dT_{rr}}{dr} + 2\frac{T_{rr} - T_{\theta\theta}}{r} = 0. \tag{28}$$

It may be observed from (14) that the mapping from R to r is one-to-one. Therefore, the statement of equilibrium (28) can be expressed in terms of the reference coordinate R as

$$\frac{dT_{rr}}{dR} + 2\frac{T_{rr} - T_{\theta\theta}}{R\lambda^3} = 0, \tag{29}$$

where $\lambda = r/R$ and (9) have been used. Written in terms of the normal stress difference, (29) becomes

$$\frac{dT_{rr}}{dR} - 2\frac{\overline{T}}{R\lambda^3} = 0. \tag{30}$$

Since the deformation is controllable, the equilibrium condition (30) is satisfied at every point $R \in [R_i, R_o]$ and at every value of the deformation control parameter λ_i.

The radial normal stress T_{rr} must be continuous and have a continuous first derivative dT_{rr}/dR on $[R_i, R_o]$. In particular, these quantities must be continuous at the interface $R = R_a$ between the inner region of converting material and the outer region composed entirely of original material. Comparison of the expressions (21) and (24) confirms that the extra stresses $\mathcal{T}_{rr}$ and $\mathcal{T}_{\theta\theta}$ are continuous at $R = R_a$ for any form of $a(s)$. It can be shown from (14), (21), (24), and (30) that $a(s_a) = 0$ and $db/ds = 0$ at $s = s_a$ are sufficient conditions for continuity of dT_{rr}/dR at $R = R_a$. These conditions will be enforced through appropriate selection of $a(s)$ and $b(s)$.

3.4. *Load-expansion relation.* Let (30) be integrated from R_i to R_o. Imposing the boundary conditions that the surface of the inner cavity be traction-free and the uniform radial tensile traction at the outer surface be T_o gives the result

$$T_o = 2\int_{R_i}^{R_o} \frac{\overline{T}}{R\lambda^3} dR. \tag{31}$$

When $\lambda_i < \lambda_a$, $s < s_a$ for $R \in [R_i, R_o]$ and T_o is found from (31), with $\overline{T} = \overline{T}^{(1)}$ given by (22). If $\lambda_i \geq \lambda_a$, microstructural transformation has been activated and $s \geq s_a$ on the inner region of the sphere $R \in [R_i, R_a]$. The external traction is then

$$T_o = 2\left[\int_{R_i}^{R_a} \frac{\overline{T}}{R\lambda^3} dR + \int_{R_a}^{R_o} \frac{\overline{T}^{(1)}}{R\lambda^3} dR\right]. \tag{32}$$

$\overline{T}$ is the current stress difference in material undergoing conversion and is given by (25). Note from (22) and (25) that $\overline{T}$ is determined at each particle R by the current value of $\lambda(R)$ and the history of $\lambda(R)$. During a process of monotonically increasing deformation, this history is identical for any particles sharing a specified current value of λ. Furthermore, the distribution $\lambda(R)$ is determined by λ_i and R_i in (14). Thus, with R_o specified, it follows from (31) that $T_o = T_o(\lambda_i)$, a relation between the traction at the outer surface and the equal biaxial stretch ratio at the inner surface of the sphere.

4. Monotonicity of response. The influence of microstructural change on the monotonicity of the T_o-λ_i relation is now investigated. It may be noted that it is because of the possibility of non-monotonic T_o-λ_i behavior that the deformation-control process of increasing λ_i has not been identified with a process of increasing T_o: the term "loading" has not been used.

The analysis presented in this section follows the approach developed by Carroll [1987] in his study of pressure maxima in the inflation of hollow spheres of a homogeneous, isotropic, incompressible nonlinear elastic material. The method presented by Carroll for uniaxial extension is borrowed, while all details of the analysis are formulated specifically for equal biaxial extension. It is easy to show that the two treatments based on uniaxial compression or equal biaxial extension are equivalent.

It is useful first to outline Carroll's analysis to set the stage for its application to materials undergoing network conversion. Since an analysis along these lines involves the visualization and comparison of several interdependent quantities, it is first presented in a simple form, with the assumption that the sphere is composed of a single material that remains elastic at all ranges of deformation. Modifications due to the occurrence of microstructural transformation and the resulting spatial variation of material properties are most easily introduced after the entire approach has been explained.

4.1. *Elastic materials.* The relation between T_o and λ_i for an elastic sphere is presented in (31), with $\overline{T} = \overline{T}^{(1)}$ given by (22). To determine whether this relation is monotonic or non-monotonic, consider the derivative $dT_o/d\lambda_i$. Note that the stress difference $\overline{T}$ in (22) can be written as $\overline{T}(\lambda(R))$. When λ_i is specified, λ is monotonic in R by (14) and it is possible to change the variable of integration and write (31) as

$$T_o = 2\int_{\lambda_i}^{\lambda_o} \frac{\overline{T}}{R\lambda^3}\frac{dR}{d\lambda}d\lambda. \tag{33}$$

Here a prescribed value of $R = R_o$ has been substituted into (14) to give

$$\lambda_o = \lambda(R_o) = \left[1 + (\lambda_i^3 - 1)\left(\frac{R_i}{R_o}\right)^3\right]^{1/3}. \tag{34}$$

Since R_i/R_o is fixed, λ_o can be considered a function of λ_i, or $\lambda_o = \lambda_o(\lambda_i)$. The function $R(\lambda)$ can be found from the one-to-one relation (14), by which $dR/d\lambda$ is formed as

$$\frac{dR}{d\lambda} = -\frac{R^4\lambda^2}{(\lambda_i^3 - 1)R_i^3}. \tag{35}$$

With (34) and (35), (33) becomes

$$T_o = -2\int_{\lambda_i}^{\lambda_o} \frac{\overline{T}}{\lambda(\lambda^3 - 1)}d\lambda. \tag{36}$$

The advantage of this form is that dependence on λ_i has been eliminated from the integrand. Differentiation of (36) with respect to λ_i gives

$$\frac{dT_o}{d\lambda_i} = 2\left[\frac{\overline{T}(\lambda_i)}{\lambda_i(\lambda_i^3 - 1)} - \frac{\overline{T}(\lambda_o)}{\lambda_o(\lambda_o^3 - 1)}\frac{d\lambda_o}{d\lambda_i}\right]. \tag{37}$$

From (34), it can be seen that

$$\frac{d\lambda_o}{d\lambda_i} = \frac{R_i^3\lambda_i^2}{R_o^3\lambda_o^2}. \tag{38}$$

Equation (34) also provides the identity

$$R_o^3(\lambda_o^3 - 1) = R_i^3(\lambda_i^3 - 1). \tag{39}$$

Substitution of (38) and (39) into (37) then gives

$$\frac{dT_o}{d\lambda_i} = \frac{2\lambda_i^2}{\lambda_i^3 - 1}\left[\frac{\overline{T}(\lambda_i)}{\lambda_i^3} - \frac{\overline{T}(\lambda_o)}{\lambda_o^3}\right]. \tag{40}$$

Introducing the notation $g = g(\lambda) = \overline{T}/\lambda^3$, (40) is further simplified to

$$\frac{dT_o}{d\lambda_i} = \frac{2\lambda_i^2}{\lambda_i^3 - 1}[g(\lambda_i) - g(\lambda_o)]. \tag{41}$$

When the sphere is composed of material that remains elastic in all deformation regimes, a single function g holds for all λ.

From (41), it can be seen that the slope of the T_o-λ_i curve vanishes and a loss of monotonicity arises when $g(\lambda_i) = g(\lambda_o)$. Information about the second derivative $d^2T_o/d\lambda_i^2$ at these critical points is also useful to the study of monotonicity. When the second derivative is evaluated with $g(\lambda_i) = g(\lambda_o)$, it takes the form

$$\frac{d^2T_o}{d\lambda_i^2} = \frac{2\lambda_i^2}{\lambda_i^3 - 1}\left[\frac{dg(\lambda_i)}{d\lambda_i} - \frac{dg(\lambda_o)}{d\lambda_i}\right]. \tag{42}$$

Since it is solely the function g that determines monotonicity, it is important to understand its properties. As is evident from its definition, $g(\lambda)$ represents an interaction of the normal stress difference $\overline{T} = \overline{T}(\lambda)$ and the kinematic quantity λ^3. For elastic materials, the expression of the stress difference as a function of λ is given by (22). $\overline{T}$ may be monotonic or nonmonotonic in λ. It is seen from (34) that $\lambda_o^3 < \lambda_i^3$, since $R_i/R_o < 1$. Furthermore, the difference between λ_o^3 and λ_i^3 is determined by the geometric factor R_i/R_o. Thus the condition $g(\lambda_i) = g(\lambda_o)$ depends in general not only on the model chosen to represent the normal stress difference $\overline{T}(\lambda)$, but also on the relative size of the cavity contained within the sphere.

The general shape of $g(\lambda)$ is first considered. Values of the stretch ratio in equal biaxial extension fall in the range $\lambda \geq 1$. As can readily be seen from (22), $\overline{T} = 0$ gives $g = 0$ at $\lambda = 1$. As λ increases from $\lambda = 1$, g increases. The behavior of g at larger λ depends on whether $\overline{T}$ increases as rapidly as $1/\lambda^3$ decreases. Carroll identified three qualitative types of material behavior which correspond to g-λ curves of three different general shapes. Examples of the general forms of such curves are presented in Fig. 2. In "type A" materials, the stress difference $\overline{T}$ increases more rapidly than λ^3 for all $\lambda \geq 1$, so that g increases monotonically with λ. In "type B" materials, $\overline{T}$ increases more rapidly than λ^3 for small λ, but g reaches a local maximum and then decreases as $1/\lambda^3$ dominates at larger λ. In "type C" materials, $\overline{T}$ is dominant as g increases for small λ; $1/\lambda^3$ dominates to cause g to decrease on some intermediate range of values of λ; then $\overline{T}$ reasserts the increasing trend at large λ. Thus the g-λ curve for "type C" materials has a local maximum followed by a local minimum.

To investigate the possibility that the non-monotonicity condition $g(\lambda_i) = g(\lambda_o)$ be satisfied, two curves may be plotted on the same set of axes for each material type. The first is $g(\lambda_i)$. For each value of λ_i, a corresponding value $\lambda_o(\lambda_i)$ is given by (34). g is evaluated at $\lambda_o(\lambda_i)$ to obtain $g(\lambda_o)$, which is plotted at λ_i to form the second curve. From (34), it is found that $\lambda_o = 1$ when $\lambda_i = 1$; so both curves share the point $(1, 0)$. $g(\lambda_o)$ takes the same basic shape as $g(\lambda_i)$, but it is "stretched" by the change of arguments

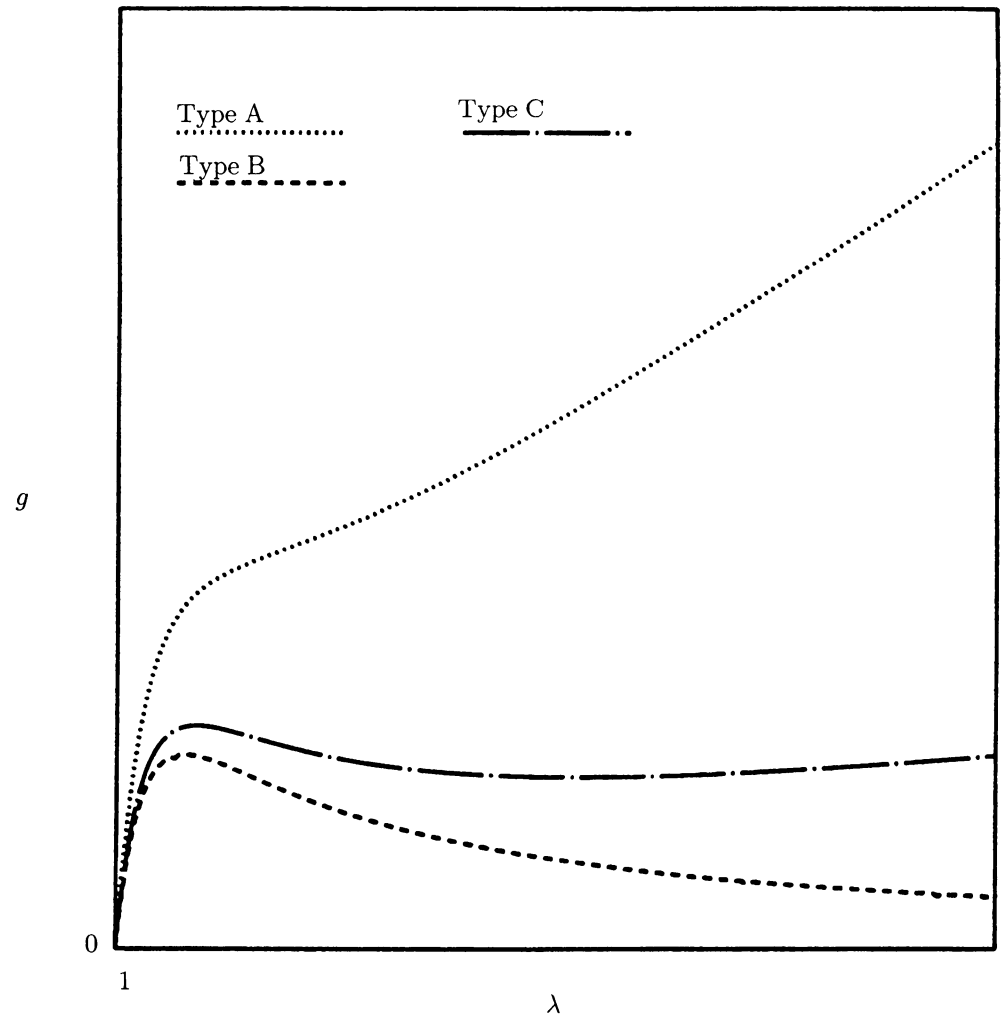

FIG. 2. Typical forms of g vs. stretch ratio for "type A", "type B", and "type C" materials

from λ_i to $\lambda_o(\lambda_i)$. Since $\lambda_o < \lambda_i$ always holds, this "stretch" of $g(\lambda_o)$ is always to the right when $g(\lambda_o)$ is plotted at λ_i. The severity of the "stretch" is determined in (34) by the geometric parameter R_i/R_o. The values of $g(\lambda_o)$ at any relative maxima or minima are the same as those of $g(\lambda_i)$.

Figure 3 shows a typical pair of plots for a "type A" material. For all values of the deformation control parameter $\lambda_i \geq 1$, the g-λ_o curve lies below the g-λ_i curve. There is no value of λ_i for which $g(\lambda_i) = g(\lambda_o)$. Thus the T_o-λ_i relation is monotonic for a homogeneous sphere composed of any "type A" material, regardless of the value of the geometric ratio R_i/R_o.

Figure 4 shows qualitative plots for a material of "type B". As the control parameter increases from $\lambda_i = 1$, $g(\lambda_i) > g(\lambda_o)$ holds. From (41), this is seen to correspond to

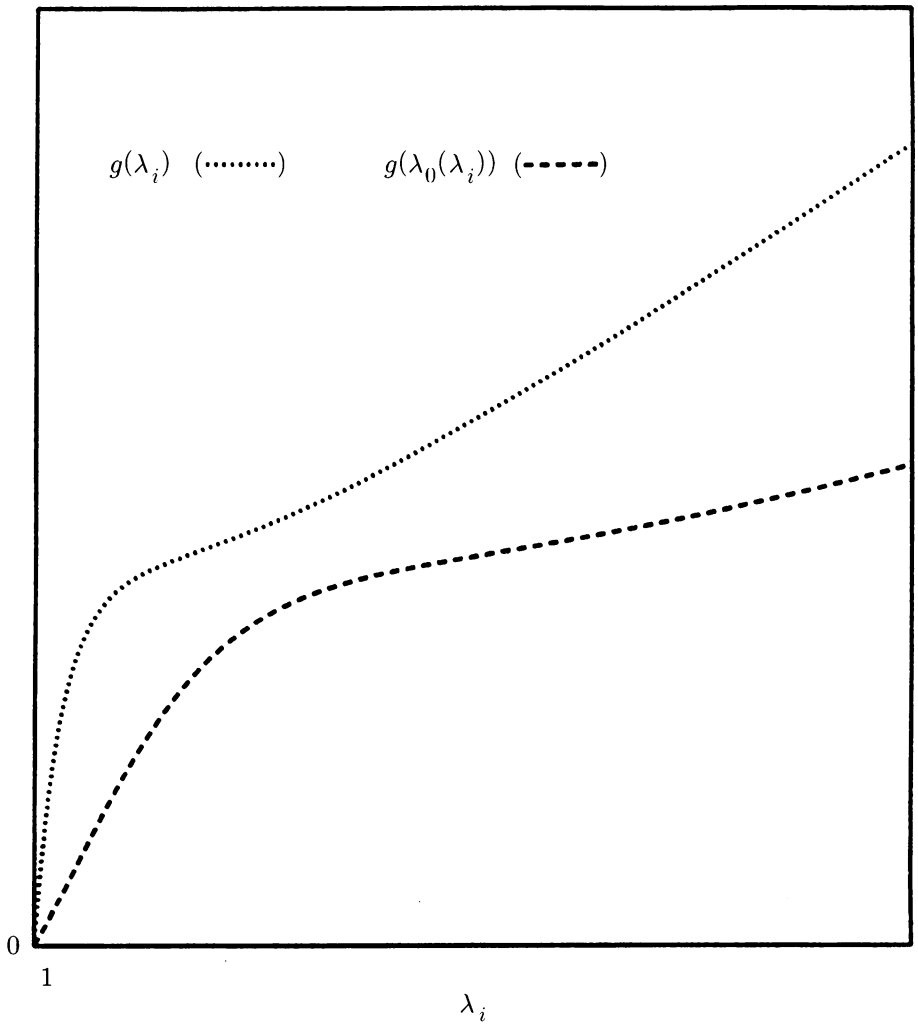

FIG. 3. Typical forms of g evaluated at inner and outer surfaces of sphere vs. inner surface stretch ratio for "type A" material

$dT_o/d\lambda_i > 0$. At a critical value of $\lambda_i = \lambda_i^{cr}$, the two curves intersect. Let $\lambda_o^{cr} = \lambda_o(\lambda_i^{cr})$. With $g(\lambda_i^{cr}) = g(\lambda_o^{cr})$, (41) gives $dT_o/d\lambda_i = 0$ at $\lambda_i = \lambda_i^{cr}$. $g(\lambda_i) < g(\lambda_o)$ then holds for $\lambda_i > \lambda_i^{cr}$, which (41) identifies with $dT_o/d\lambda_i < 0$. Thus there is a single local maximum in the T_o-λ_i curve at $\lambda_i = \lambda_i^{cr}$. This observation is supported by consideration of the second derivative $d^2T_o/d\lambda_i^2$ at $\lambda_i = \lambda_i^{cr}$. As can be seen from (41), the factor $2\lambda_i^2/(\lambda_i^3 - 1) > 0$ for all $\lambda_i > 1$. Inspection of Fig. 4 reveals that the slope $dg(\lambda_i)/d\lambda_i < 0$ at $\lambda_i = \lambda_i^{cr}$, while $dg(\lambda_o)/d\lambda_i > 0$. Thus (42) gives $d^2T_o/d\lambda_i^2 < 0$, confirming that there is a local maximum in the T_o-λ_i curve at $\lambda_i = \lambda_i^{cr}$. It should be noted that the value of λ_i^{cr} can be made lesser or greater by adjusting the ratio R_i/R_o. However, there always exists a point of intersection of the two curves and hence a local maximum arises in the T_o-λ_i relation for spheres composed of "type B" material.

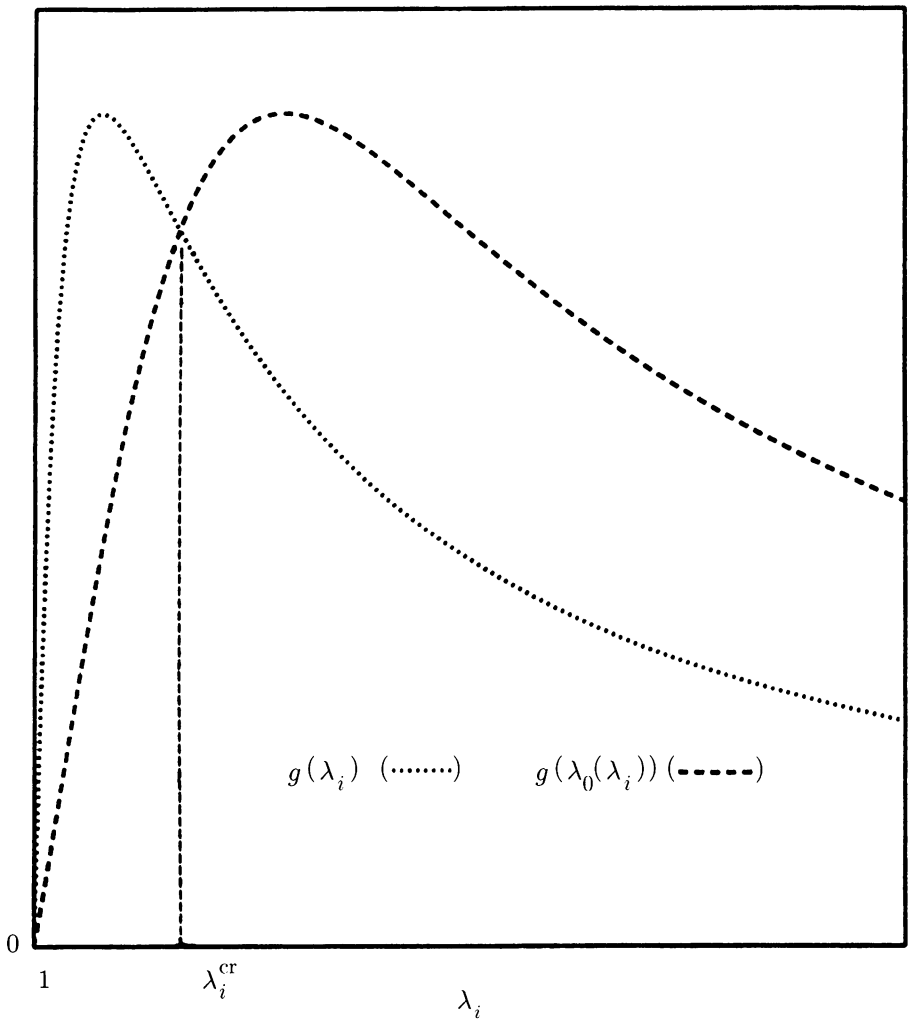

FIG. 4. Typical forms of g evaluated at inner and outer surfaces of sphere vs. inner surface stretch ratio for "type B" material

Figure 5 shows plots of $g(\lambda_i)$ and $g(\lambda_o)$ for materials of "type C". It can be seen that the existence of points of intersection is not guaranteed for all spheres composed of "type C" materials. For sufficiently thick-walled spheres, $R_i/R_o \ll 1$. From (34), $\lambda_o \ll \lambda_i$ and the "stretch" of $g(\lambda_o)$ relative to $g(\lambda_i)$ can be so great that $g(\lambda_o)$ lies everywhere below $g(\lambda_i)$, with no intersection. Then there is no value of λ_i at which $dT_o/d\lambda_i = 0$ and the T_o-λ_i curve is monotonic. For sufficiently thin-walled spheres, R_i/R_o is closer to unity, which indicates a small shift from λ_i to λ_o. As can be seen in Fig. 5, it is then possible that $g(\lambda_i)$ and $g(\lambda_o)$ intersect. In fact, intersection can occur at two points. From Fig. 5 and the expressions (41) and (42) for the first and second derivatives it is seen that $d^2T_o/d\lambda_i^2 < 0$ at $\lambda_i = \lambda_i^{cr\,1}$ and $d^2T_o/d\lambda_i^2 > 0$ at $\lambda_i = \lambda_i^{cr\,2}$. Thus T_o has a local maximum at $\lambda_i^{cr\,1}$ and a local minimum at $\lambda_i^{cr\,2}$. For spheres of "type C" material,

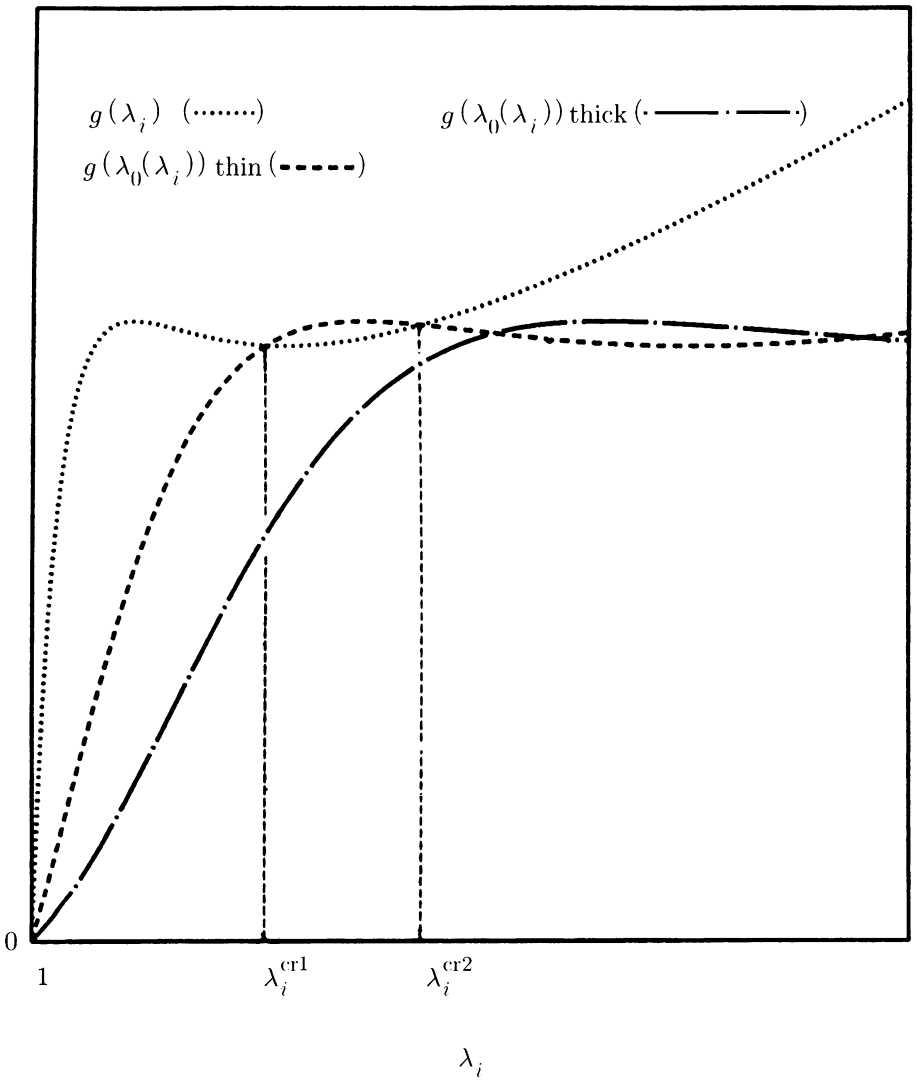

FIG. 5. Typical forms of g evaluated at inner and outer surfaces of sphere vs. inner surface stretch ratio for "type C" material

the ratio of radii R_i/R_o determines whether the T_o-λ_i curve is monotonic or has a local maximum followed by a local minimum.

4.2. *Materials undergoing microstructural change.* Now that a framework for the analysis of the T_o-λ_i behavior of homogeneous spheres has been constructed, the variation introduced by the constitutive equation for materials undergoing microstructural change can be addressed. Attention is focused on values of the control parameter λ_i for which there exists an $R_a \in (R_i, R_o)$: material of the inner portion of the sphere, $R \in [R_i, R_a]$, has undergone microstructural conversion, but the outer region, $R \in [R_a, R_o]$, is composed entirely of original-network material. While Carroll's analysis assumes that a

single function g applies for all $\lambda \geq 1$, different expressions are now in general required at $\lambda = \lambda_i$ and $\lambda = \lambda_o$.

The expression for T_o when network transformation is occurring in the inner portion of the sphere is given by (32). As discussed in Sec. 4.1, $\overline{T}^{(1)}$ in (22) is regarded as a function of λ. Since $s = s(\lambda)$, $\overline{T}$ in (25) can also be regarded as a function of λ. For each fixed value of λ_i, it is again possible to change the independent variable of integration from R to λ. When this change of variable is introduced, (32) may be written as

$$T_o = -2\left[\int_{\lambda_i}^{\lambda_a} \frac{\overline{T}}{\lambda(\lambda^3-1)}d\lambda + \int_{\lambda_a}^{\lambda_o} \frac{\overline{T}^{(1)}}{\lambda(\lambda^3-1)}d\lambda\right], \tag{43}$$

where $\overline{T}^{(1)}$, given by (22), is the stress difference in the purely elastic material of the region $R \in [R_a, R_o]$ and $\overline{T}$, given by (25), is the stress difference in the conversion region $R \in [R_i, R_a]$. It can be seen from Sec. 3.2 that $\overline{T}$ is continuous at λ_a. The derivative $dT_o/d\lambda_i$ is formed from (43) as

$$\frac{dT_o}{d\lambda_i} = \frac{2\lambda_i^2}{\lambda_i^3-1}\left[\frac{\overline{T}(\lambda_i)}{\lambda_i^3} - \frac{\overline{T}^{(1)}(\lambda_o)}{\lambda_o^3}\right], \tag{44}$$

with λ_o given by (34). Introduce the notation $g^{(1)}(\lambda) = \overline{T}^{(1)}(\lambda)/\lambda^3$, the form of g appropriate to elastic material that has not undergone conversion. The condition that implies $dT_o/d\lambda_i = 0$ and hence a loss of monotonicity becomes $g(\lambda_i) = g^{(1)}(\lambda_o)$.

A new set of figures analogous to those discussed above can be constructed in order to investigate whether the T_o-λ_i relation is monotonic or otherwise when network conversion occurs. Before doing so, the restriction is made that the case of network conversion is considered to imply material softening. Thus

$$\overline{T}(\lambda) \begin{cases} = \overline{T}^{(1)}(\lambda), & \lambda < \lambda_a, \\ < \overline{T}^{(1)}(\lambda), & \lambda > \lambda_a. \end{cases} \tag{45}$$

It should be understood that plots can be constructed for cases of either conversion-softening or conversion-hardening. The above restriction is imposed in the interest of brevity.

Figure 6 shows $g(\lambda_i)$ vs. λ_i and $g^{(1)}(\lambda_o)$ vs. λ_i for material of "type B". The $g^{(1)}(\lambda_i)$ vs. λ_i curve is also plotted to aid in the construction of $g^{(1)}(\lambda_o)$ and for comparison with $g(\lambda_i)$. Note that $g^{(1)}(\lambda)$ is not the appropriate function for use at $\lambda = \lambda_i$, within the region of the sphere where network conversion is under way. The function $g^{(1)}(\lambda_o)$ is formed from $g^{(1)}(\lambda_i)$ as above and plotted as a function of λ_i. Again the "stretching" of $g^{(1)}(\lambda_i)$ to the right to form $g^{(1)}(\lambda_o)$ is due to the geometric shift from λ_i to λ_o. A point of intersection of $g^{(1)}(\lambda_o)$ with $g^{(1)}(\lambda_i)$ is seen at $\lambda_i = \lambda_i^{\mathrm{cr}'}$. This is the value of the control parameter at which $dT_o/d\lambda_i = 0$ would hold if the sphere were homogeneous, composed entirely of non-converting elastic material.

As required by (45) and as can be seen in Fig. 6, $g(\lambda_i)$ lies below $g^{(1)}(\lambda_i)$ for $\lambda_i > \lambda_a$. In general, then, these two curves intersect $g^{(1)}(\lambda_o)$ at different values of λ_i. In the case of the conversion softening of a "type B" material, it appears from Fig. 6 that $\lambda_i^{\mathrm{cr}} < \lambda_i^{\mathrm{cr}'}$. Thus the T_o-λ_i relation may be seen to lose monotonicity at a lower value of

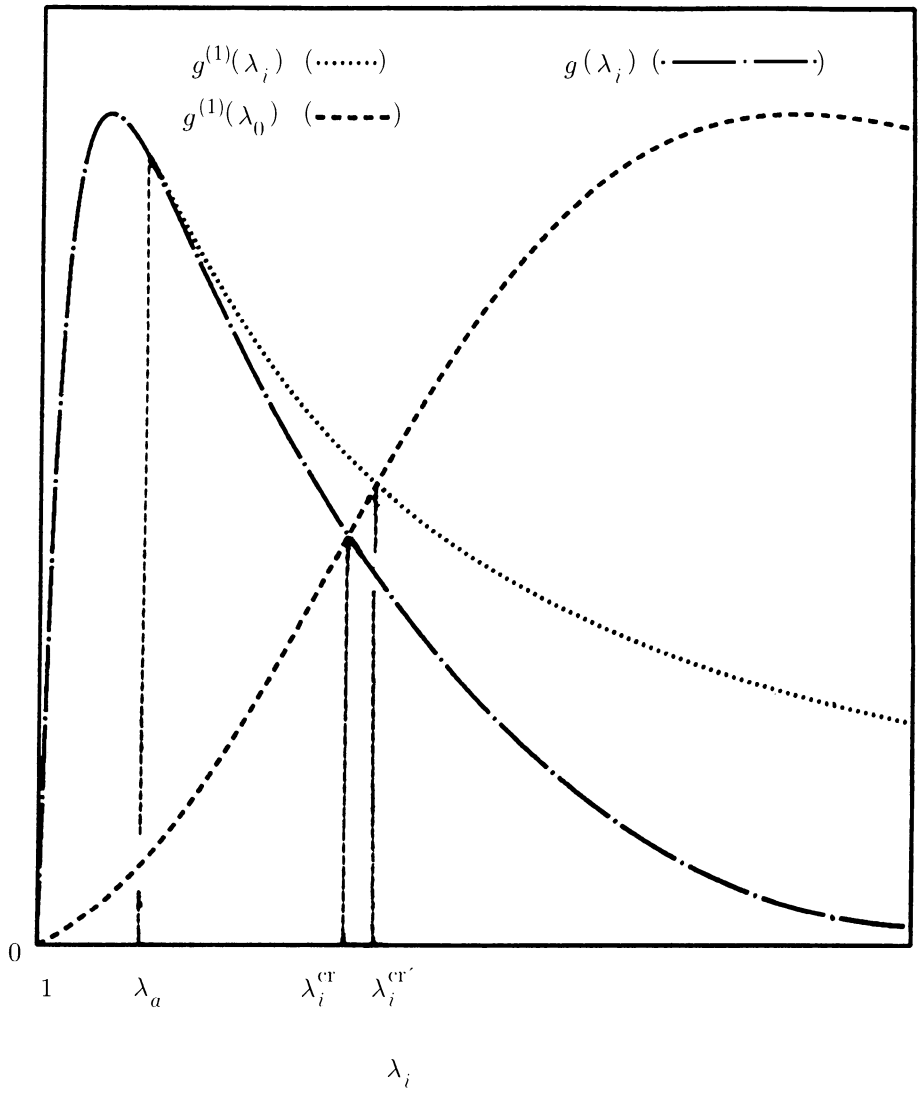

FIG. 6. Typical forms of g evaluated at inner and outer surfaces of sphere vs. inner surface stretch ratio for "type B" and conversion-softening materials

λ_i when conversion-softening is assumed to occur than would be the case for a sphere of homogeneous "type B" material.

Figure 7 shows $g(\lambda_i)$ vs. λ_i, $g^{(1)}(\lambda_o)$ vs. λ_i and $g^{(1)}(\lambda_i)$ vs. λ_i for a typical "type A" material when microstructural conversion is assumed to induce softening of response. Although $g^{(1)}(\lambda_i)$ does not appear in the monotonicity condition when the material of the sphere undergoes network conversion, it is shown for purposes of comparison. The function $g^{(1)}(\lambda_o)$ is plotted as the result of the geometric shift from λ_i to λ_o and lies everywhere below $g^{(1)}(\lambda_i)$. The only restriction on $g(\lambda_i)$ is that it lie below $g^{(1)}(\lambda_i)$ for

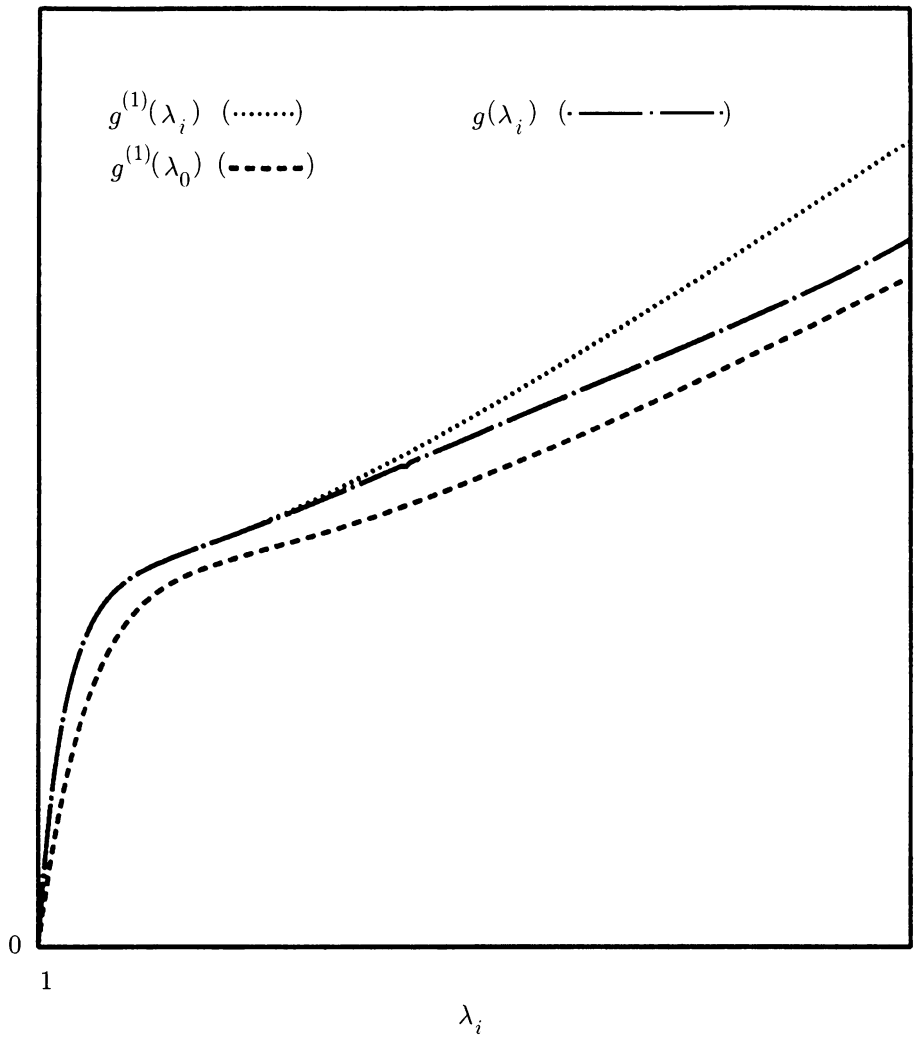

FIG. 7. Typical forms of g evaluated at inner and outer surfaces of sphere vs. inner surface stretch ratio for "type A" and "mild" conversion-softening materials

$\lambda_i > \lambda_a$. In Fig. 7, conversion-softening has been "mild", so that the converted material still shows "type A" behavior and $g(\lambda_i)$ and $g^{(1)}(\lambda_o)$ do not intersect. Consequently, there is no loss of monotonicity.

Figures 8 through 10 show possible results for a "type A" material when conversion-softening is more "severe". As seen in all three figures, it is possible that there exist points of intersection of $g(\lambda_i)$ and $g^{(1)}(\lambda_o)$. Figure 8 shows a case where the converting material remains "type A". In Fig. 9 there is "type B" response. In Fig. 10, the converting material demonstrates "type C" response. In each of the three cases, the condition for $dT_o/d\lambda_i = 0$ is satisfied at some $\lambda_i = \lambda_i^{\text{cr}}$. The assumption of deformation-induced

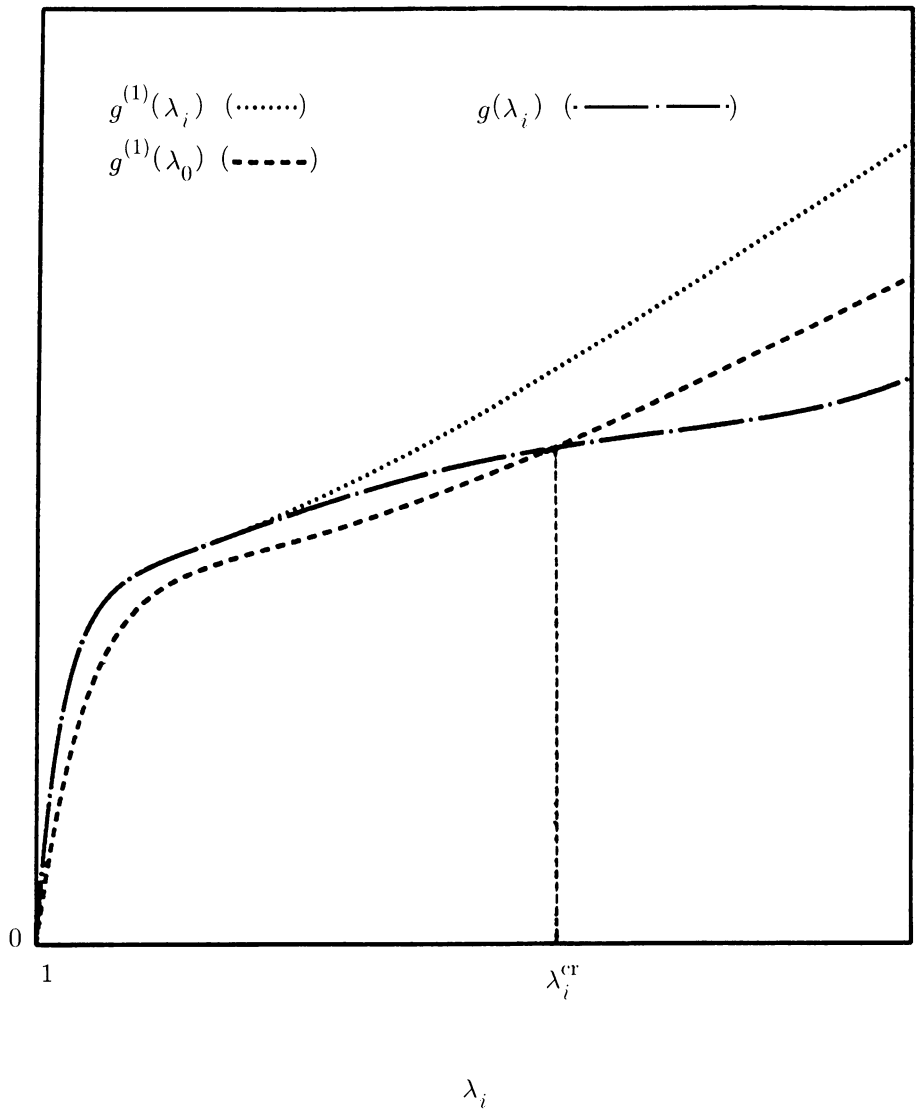

FIG. 8. Typical forms of g evaluated at inner and outer surfaces of sphere vs. inner surface stretch ratio for "type A" material and conversion-softening material with "type A" response

microstructural transformation makes possible a loss of monotonicity of T_o vs. λ_i which cannot otherwise occur in "type A" materials.

Depending on the value of the geometric factor R_i/R_o, spheres composed of "type C" materials may exhibit monotonic or non-monotonic T_o-λ_i behavior. This explicit geometric influence requires the consideration of many more possible cases than for materials of "type A" and "type B". These cases may be studied as above. Since no new ideas are introduced, these effects are not presented graphically. It is proposed without demonstration that the assumption of microstructural transformation can exert the

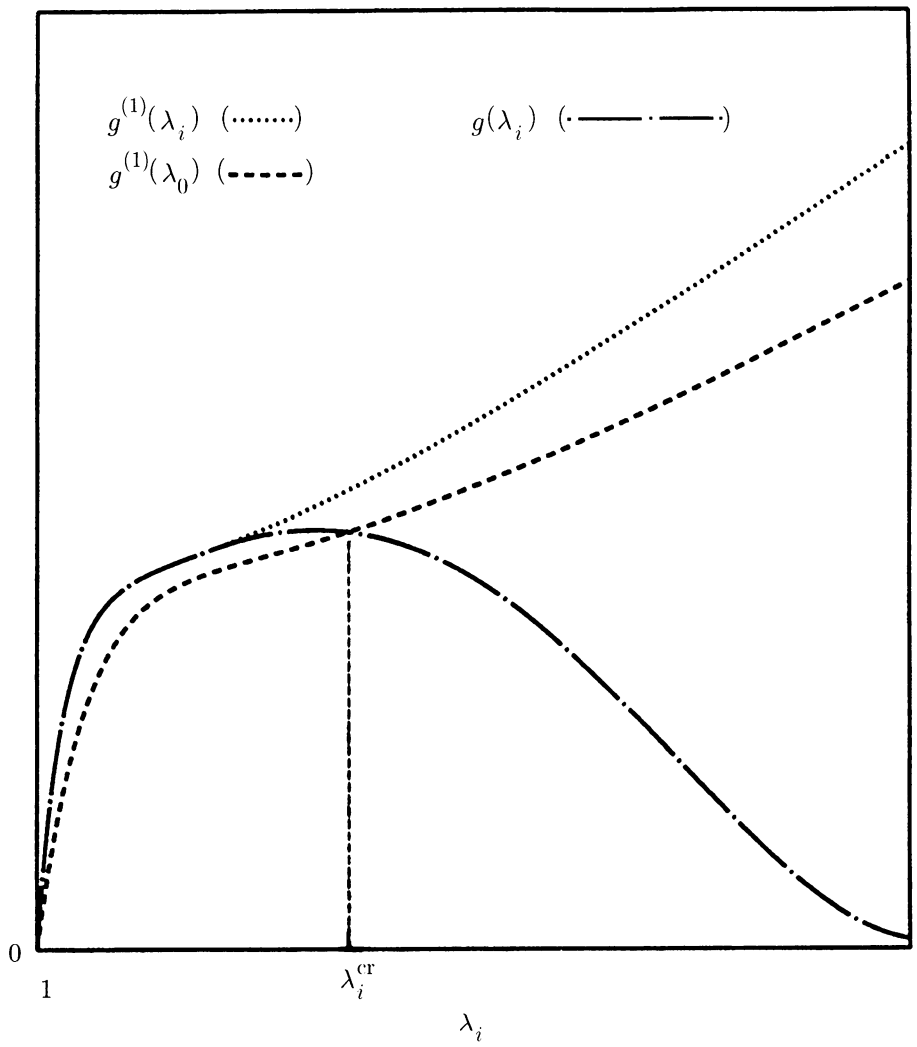

FIG. 9. Typical forms of g evaluated at inner and outer surfaces of sphere vs. inner surface stretch ratio for "type A" material and conversion-softening material with "type B" response

same sort of influence as has been seen in Figs. 6 through 10. For values of R_i/R_o at which the homogeneous sphere of "type C" material has a non-monotonic T_o-λ_i relation, conversion can alter the values of λ_i at which the local maxima and minima occur. For values of R_i/R_o at which a "type C" homogeneous sphere cannot demonstrate a loss of monotonicity, the assumption of conversion can make such non-monotonicity possible.

At this juncture, it is worth noting that an "equivalent elastic" material could be considered, whose stress-stretch relation is given by combining the domains of definition of $\overline{T}^{(1)}$ and $\overline{T}$. For such an "equivalent elastic" material, Carroll's analysis would apply. However, it cannot be overemphasized that the present stress-stretch relation is not for

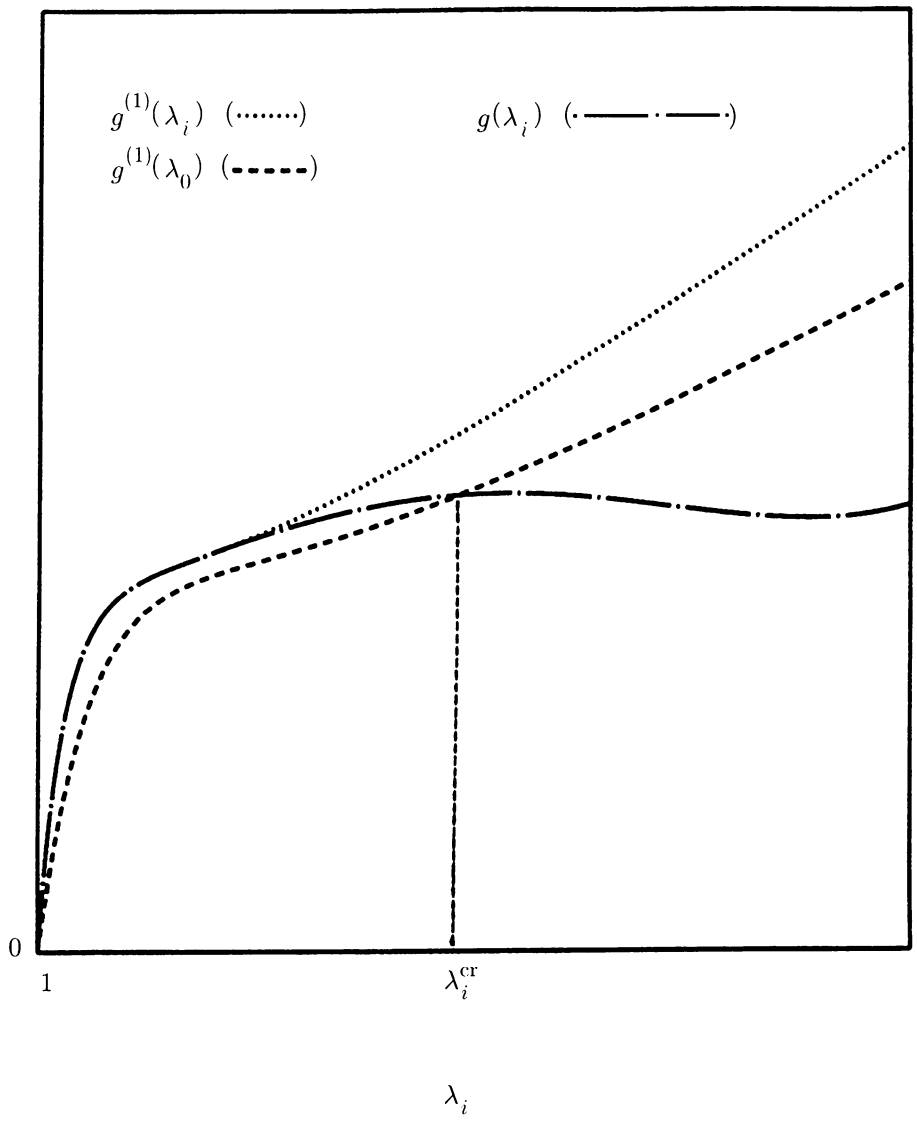

FIG. 10. Typical forms of g evaluated at inner and outer surfaces of sphere vs. inner surface stretch ratio for "type A" material and conversion-softening material with "type C" response

a single elastic body. This fact becomes obvious when the body is unloaded (Huntley, Wineman, and Rajagopal [1996]).

The general methodology for studying the possibilities of non-monotonic T_o-λ_i behavior in the context of the present constitutive equation has been presented in this section. Specific applications are carried out below.

5. Numerical solution. In order to carry out a numerical solution, specific choices must be made for two material properties—the deformation state function s and the conversion rate function $a(s)$ introduced in (3). The deformation state function is chosen as $s = \lambda$ for $\lambda \geq 1$. Since the stretch ratio varies with the radius R, so does the state parameter; hence $s(R) = \lambda(R)$. The conversion activation criterion is satisfied for the particle at radius R when $s(R) = \lambda(R) = \lambda_a$. The activation radius, then, is defined by $\lambda(R_a) = \lambda_a$.

The conversion rate function $a(\lambda) = a(s)$ is chosen to be quadratic on a finite domain:

$$a(\lambda) = \begin{cases} 0, & \lambda < \lambda_a, \\ \alpha(\lambda - \lambda_a)(\lambda - \lambda_c), & \lambda \in [\lambda_a, \lambda_c], \\ 0, & \lambda > \lambda_c. \end{cases} \tag{46}$$

According to this definition of $a(\lambda)$, the process of material conversion occurs as the deformation state parameter λ increases over a finite interval and the process terminates when $\lambda > \lambda_c$. Since the deformations under consideration are finite, the parameter λ will not exceed some finite value. Thus, λ_c can be chosen sufficiently large that, in the present examples, the conversion process need not reach completion. (It should be noted that other choices of $a(\lambda)$ can be made in which λ_c is not finite.)

In virtue of the incompressibility of the material, the rate of decrease of volume fraction of original material equals the rate of increase of volume fraction of material with new microstructure. This implies that the volume fraction of original material remaining at any state of deformation $\lambda > \lambda_a$ is

$$b(\lambda) = 1 - \int_{\lambda_a}^{\lambda} a(\hat{\lambda}) d\hat{\lambda}. \tag{47}$$

With $a(\lambda)$ chosen as in (46) and $b(\lambda)$ chosen as in (47), the continuity condition for dT_{rr}/dR at $R = R_a$ is satisfied. Let the total volume fraction of material that may ultimately convert be denoted by C, where $C \leq 1$. Then by (47),

$$C = \int_{\lambda_a}^{\lambda_c} a(\hat{\lambda}) d\hat{\lambda}. \tag{48}$$

It then follows from (46) and (48) that

$$\alpha = -\frac{6C}{(\lambda_c - \lambda_a)^3}. \tag{49}$$

Values of λ_a, λ_c, and C are selected so as to make evident the differences in response between the sphere undergoing conversion and an elastic sphere (no conversion, $C = 0$). For the examples in this section, $\lambda_a = 1.5$ is chosen so that network conversion commences at a relatively low level of deformation. It is desired to continue the simulation to the level $\lambda = 6.0$. Thus $\lambda_c = 6.1$ is chosen. This permits the simulation to demonstrate the effects of conversion of nearly all of the material specified by C while not exceeding λ_c.

Define a dimensionless radial coordinate by $\widetilde{R} = R/R_i$. The equation (14) giving the stretch distribution becomes

$$\lambda = \lambda(\widetilde{R}) = \left(1 + \frac{\lambda_i^3 - 1}{\widetilde{R}^3}\right)^{1/3}. \tag{50}$$

When λ_i is specified, λ is a monotonically decreasing function of $\widetilde{R}$. The numerical examples presented below assume a sphere occupying the reference domain $\widetilde{R} \in [1.0, 10.0]$. The dimensionless outer radius of the sphere, denoted by $\widetilde{R}_o = R_o/R_i$, is thus $\widetilde{R}_o = 10$. The dimensionless activation radius $\widetilde{R}_a = R_a/R_i$ is given by

$$\widetilde{R}_a = \left(\frac{\lambda_i^3 - 1}{\lambda_a^3 - 1} \right)^{1/3}. \tag{51}$$

Here, $\widetilde{R}_a$ is undefined for $\lambda_i < \lambda_a$. $\widetilde{R}_a$ moves outward through the sphere for increasing $\lambda_i \geq \lambda_a$. At large λ_i, the plot of $\widetilde{R}_a$ vs. λ_i asymptotically approaches the straight line $\widetilde{R}_a = \lambda_i(\lambda_a^3 - 1)^{-1/3}$. The normal stress difference $\overline{T}$ and the traction T_o are normalized by an elastic constant appropriate to the material model being considered. This gives dimensionless quantities denoted by $\widetilde{T}$ and $\widetilde{T}_o$, respectively.

The numerical procedure for solution begins with the specification of a value of the deformation control parameter λ_i. Then $\lambda(\widetilde{R})$ is known everywhere from (50). With the activation stretch ratio λ_a prescribed, (51) gives $\widetilde{R}_a$. Using the quadratic form of $a(\lambda)$ specified in (46), the integral in (25) can be expanded analytically. In order to evaluate the integrals in (32), $\widetilde{R}_a$ is found from (51) and the region $[1, \widetilde{R}_a]$ is discretized to form n intervals of equal size demarcated by the nodes $\widetilde{R} = R_j$ $(j = 1, n+1)$, with $R_1 = 1$ and $R_{n+1} = \widetilde{R}_a$. Similarly, discretization of the region $[\widetilde{R}_a, \widetilde{R}_o]$ into m intervals is accomplished with the evenly spaced nodes $\widetilde{R} = R_j$ $(j = 1, m+1)$, with $R_1 = \widetilde{R}_a$ and $R_{m+1} = \widetilde{R}_o$. The integrand of (25) is then evaluated at the nodal values R_j and the integral is approximated by Simpson's rule. The two distinct discretized regions are necessary because, as is known from (32), different forms of $\widetilde{T}$ apply in the separate regions. When $\lambda_i \geq \lambda_a$, the numerical integration must be carried out from $\widetilde{R} = 1$ precisely to $\widetilde{R} = \widetilde{R}_a$ using $\widetilde{T}$ as given by (25); from $\widetilde{R} = \widetilde{R}_a$ to $\widetilde{R} = \widetilde{R}_o$, the integration by Simpson's rule continues, using the expression (22) for $\widetilde{T} = \widetilde{T}^{(1)}$.

6. Examples.

6.1. *Neo-Hookean material.* Let it be assumed that the original material of the sphere is a neo-Hookean elastic solid and that the material of each subsequently formed network also exhibits neo-Hookean response. By Carroll's classification, a neo-Hookean material is a "type B" material. Thus, this example is illustrative of the analysis associated with Fig. 6. The strain energy density functions $W^{(1)}$ and $W^{(2)}$ for the original and newly formed network materials, respectively, are taken as

$$W^{(1)}(I_1, I_2) = c^{(1)}(I_1 - 3); \qquad W^{(2)}(\hat{I}_1, \hat{I}_2) = c^{(2)}(\hat{I}_1 - 3), \tag{52}$$

where $c^{(1)}$ and $c^{(2)}$ are constants interpreted as material moduli. Comparison with (23) and (26) shows that

$$c^{(1)} = E^{(1)} = W_1^{(1)}; \qquad c^{(2)} = E^{(2)} = W_1^{(2)}. \tag{53}$$

In the present solution, $\overline{T}, \overline{T}^{(1)}$, and T_o in (32) are normalized by the modulus $E^{(1)}$. It is emphasized that the restriction to neo-Hookean network response is not necessary. Both original and subsequently formed materials are taken as neo-Hookean in order to demonstrate as clearly as possible the effects of the conversion phenomenon itself

on overall mechanical response. The possibility is allowed that the original and newly formed materials have different moduli, that is, that $E^{(1)}$ and $E^{(2)}$ may not be equal. Let $\widetilde{E} = E^{(2)}/E^{(1)}$.

Figure 11 shows the external traction $\widetilde{T}_o$ vs. λ_i for three values of the ratio of moduli $\widetilde{E}$. The conversion fraction is taken as $C = 1.0$. For comparison, the neo-Hookean case with $C = 0.0$ is represented by the solid curve. It can be seen that the external traction associated with a given value of the deformation control parameter λ_i is smaller when conversion is assumed than in the purely elastic case. It may be said in general that conversion leads to a softening of the load-expansion response of the sphere for $\lambda_i \geq \lambda_a$. Figure 11 indicates that variations of the modulus ratio over the range $\widetilde{E} \in [0.5, 2.0]$ used in this work have little noticeable influence on the $\widetilde{T}_o$-λ_i relation. For this reason, no further comparisons of response for different values of $\widetilde{E}$ are presented in this article. The value $\widetilde{E} = 1.0$ is used henceforth.

Figure 12 shows the $\widetilde{T}_o$-λ_i relation for different values of C. The softening effect is evident for $\lambda_i > \lambda_a = 1.5$ for each value of $C > 0.0$ shown and is more pronounced when C is larger.

All of the curves plotted in Fig. 12 demonstrate non-monotonic $\widetilde{T}_o$-λ_i relations. As mentioned above, Carroll categorized the neo-Hookean material as a "type B" material: in spheres of any normalized thickness $\widetilde{R}_o$, a loss of monotonicity will occur at some λ_i. Recall from Sec. 4.2 that the $\widetilde{T}_o$-λ_i relation for a conversion-softening "type B" material may lose monotonicity at a lower value of λ_i than would occur if the response were purely elastic. The local maximum of $\widetilde{T}_o$, indicated on each curve by a heavy dot, can be seen to occur at smaller λ_i and at lower values of $\widetilde{T}_o$ when C is greater. The critical value of λ_i decreases from $\lambda_i^{\mathrm{cr}} \approx 5.00$ for the neo-Hookean material to $\lambda_i^{\mathrm{cr}} \approx 4.06$ when $C = 1.0$. The external traction associated with λ_i^{cr} decreases from $\widetilde{T}_o^{\mathrm{cr}} \approx 3.90$ to $\widetilde{T}_o^{\mathrm{cr}} \approx 3.64$.

Define a dimensionless form of $g(\lambda_i)$ by $\tilde{g} = \tilde{g}(\lambda_i) = \widetilde{T}(\lambda_i)/\lambda_i^3$. Figure 13 shows $\tilde{g}$ plotted as a function of λ_i for each of the values of C considered in Fig. 12. The function appropriate to the neo-Hookean case ($C = 0.0$) is shown by the upper solid line. Superposed on this family of curves is the plot of $\tilde{g}^{(1)}(\lambda_o)$ vs. λ_i. It has been established that the intersection of $\tilde{g}^{(1)}(\lambda_o)$ with $\tilde{g}(\lambda_i)$ occurs at the value of λ_i at which the derivative $d\widetilde{T}_o/d\lambda_i$ vanishes and the $\widetilde{T}_o$-λ_i relation loses monotonicity. It can be seen from the figure that the intersection of $\tilde{g}^{(1)}(\lambda_o)$ with the $\tilde{g}(\lambda_i)$ curve occurs at a lower value of λ_i when the conversion fraction C is greater. This set of values of λ_i^{cr} for the different values of C corresponds to the set of local maxima seen in Fig. 12.

6.2. *Mooney-Rivlin material.* A brief study of $\widetilde{T}_o(\lambda_i)$ is now presented for the Mooney-Rivlin material. This model can be used to represent "type A" response by Carroll's classification. Thus, this example illustrates the analysis associated with Figs. 7 and 8.

Assume that the original microstructural networks and all subsequently formed networks behave as Mooney-Rivlin materials. The strain energy density function for materials of this type is

$$W(I_1, I_2) = c_1(I_1 - 3) + c_2(I_2 - 3), \tag{54}$$

where c_1 and c_2 are constants. For simplicity, assume that $W^{(1)} = W^{(2)} = W$. Thus, original and subsequently formed network materials have the same moduli. $\overline{T}, \overline{T}^{(1)}$, and

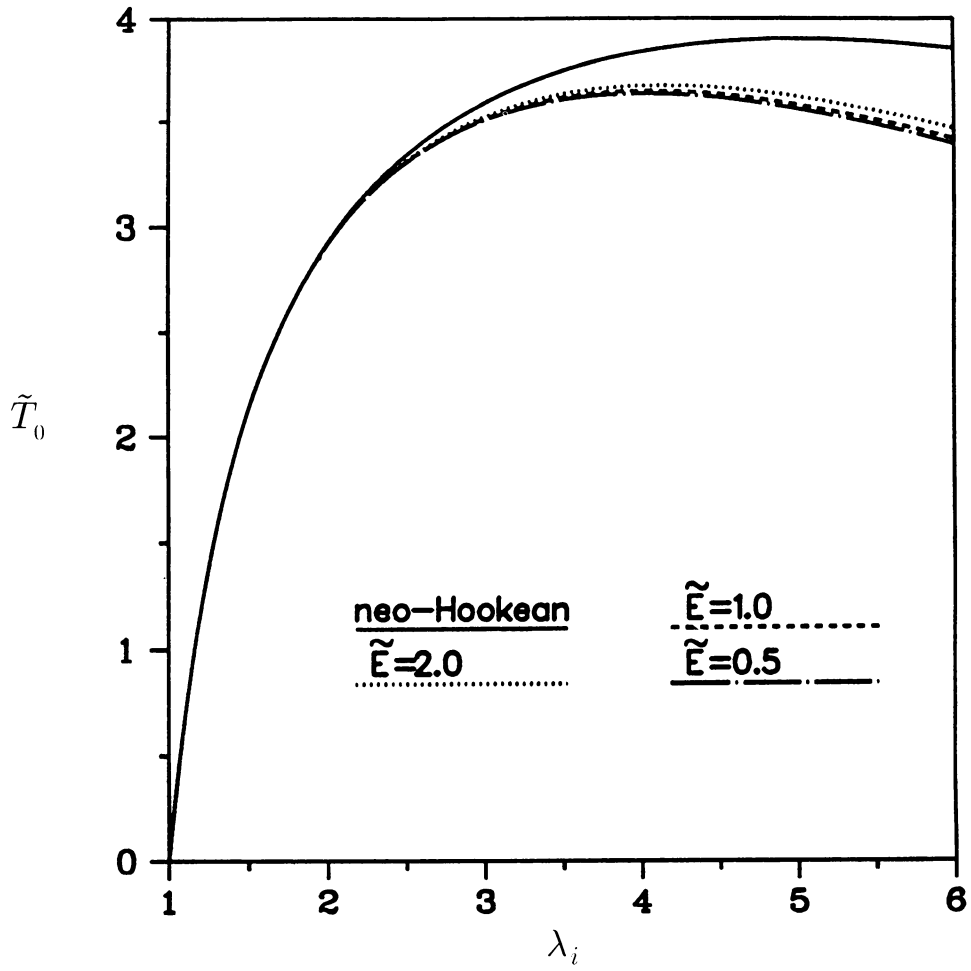

FIG. 11. External radial tensile traction vs. inner surface stretch ratio for various modulus ratios, with $\widetilde{R}_o = 10$, $C = 1.0$, $\lambda_a = 1.5$, and $\lambda_c = 6.1$

T_o in (32) are normalized by c_1. Let $\gamma = c_2/c_1$. The conversion rate function $a(s) = a(\lambda)$ and the volume fraction of original material remaining $b(s) = b(\lambda)$ are taken as those used in the study of neo-Hookean materials in Sec. 6.1.

Figure 14 shows the traction $\widetilde{T}_o$ vs. λ_i for different values of the conversion fraction C. The activation value is taken as $\lambda_a = 2.0$; conversion is considered complete at $\lambda_c = 6.1$. The dimensionless outer radius of the sphere is $\widetilde{R}_o = 4.0$. $\gamma = 0.3$ is chosen. Results for a purely elastic Mooney-Rivlin material undergoing no microstructural transformation are represented by the solid line. According to Carroll's classification, a Mooney-Rivlin material with $\gamma = 0.3$ is a "type A" material. The $\widetilde{T}_o$-λ_i relation increases monotonically for all values of λ_i. On the deformation range $\lambda_i \in [1.0, 6.0]$, the curve for $C = 0.0$ in Fig. 14 shows such monotonicity. When amounts of conversion $C > 0.0$ are assumed, material in the region $\widetilde{R} \in [1, \widetilde{R}_a]$ softens for $\lambda_i > \lambda_a = 2.0$. The traction associated with

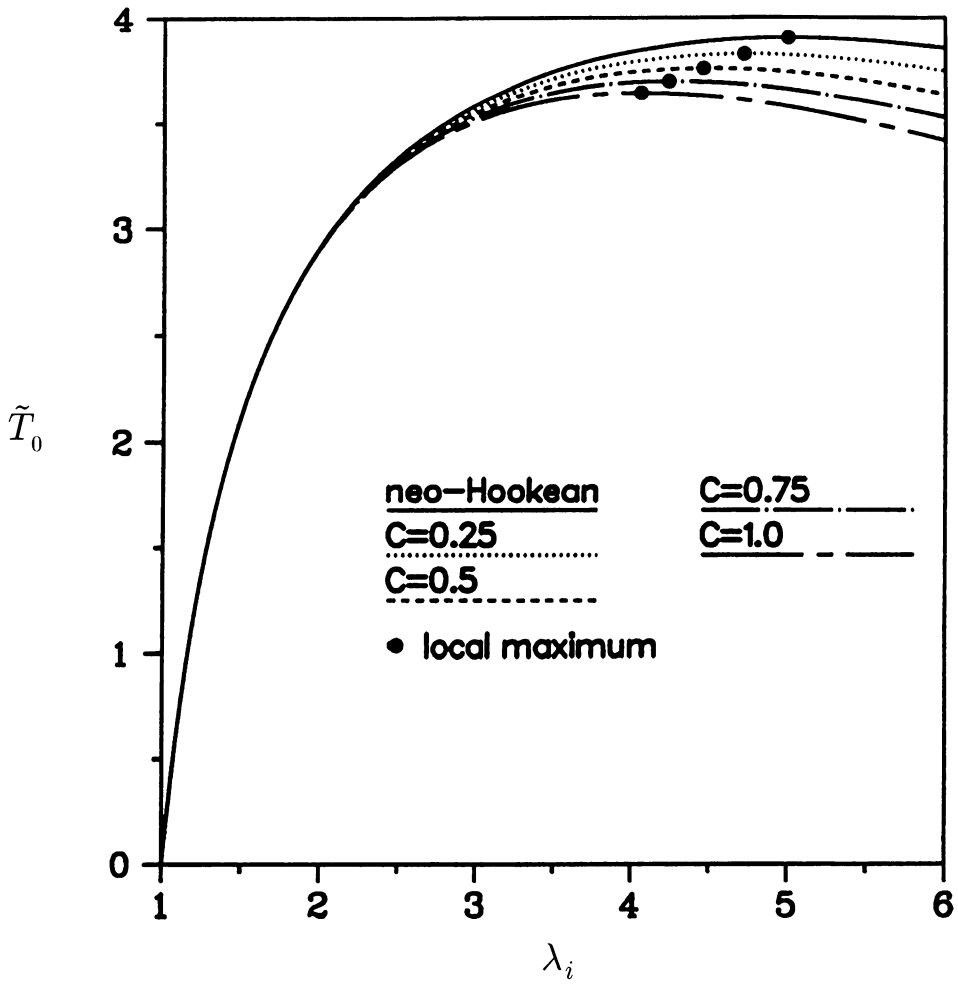

FIG. 12. External radial tensile traction vs. inner surface stretch ratio for various conversion fractions, with $\tilde{R}_o = 10$, $\tilde{E} = 1.0$, $\lambda_a = 1.5$, and $\lambda_c = 6.1$

a given value of $\lambda_i > 2.0$ is lower than in the elastic case ($C = 0.0$). When C is larger, $\tilde{T}_o$ is smaller for all $\lambda_i \in [2.0, 6.0]$. It can be seen from the figure that monotonicity is lost in the curves for $C = 0.5$, $C = 0.75$, and $C = 1.0$. Moreover, the value of λ_i at which the local maximum arises can be seen to decrease as C increases.

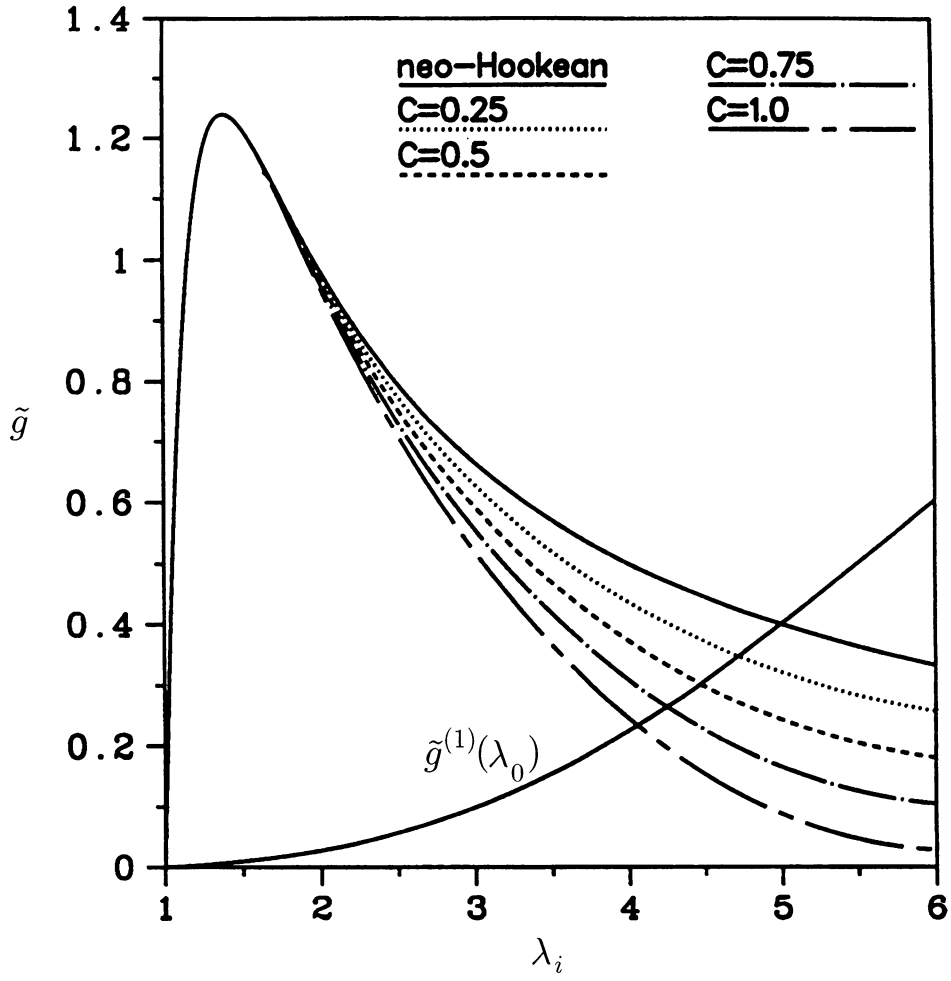

FIG. 13. g evaluated at inner and outer surfaces of sphere vs. inner stretch ratio for various conversion fractions, with $\widetilde{R}_o = 10$, $\widetilde{E} = 1.0$, $\lambda_a = 1.5$, and $\lambda_c = 6.1$

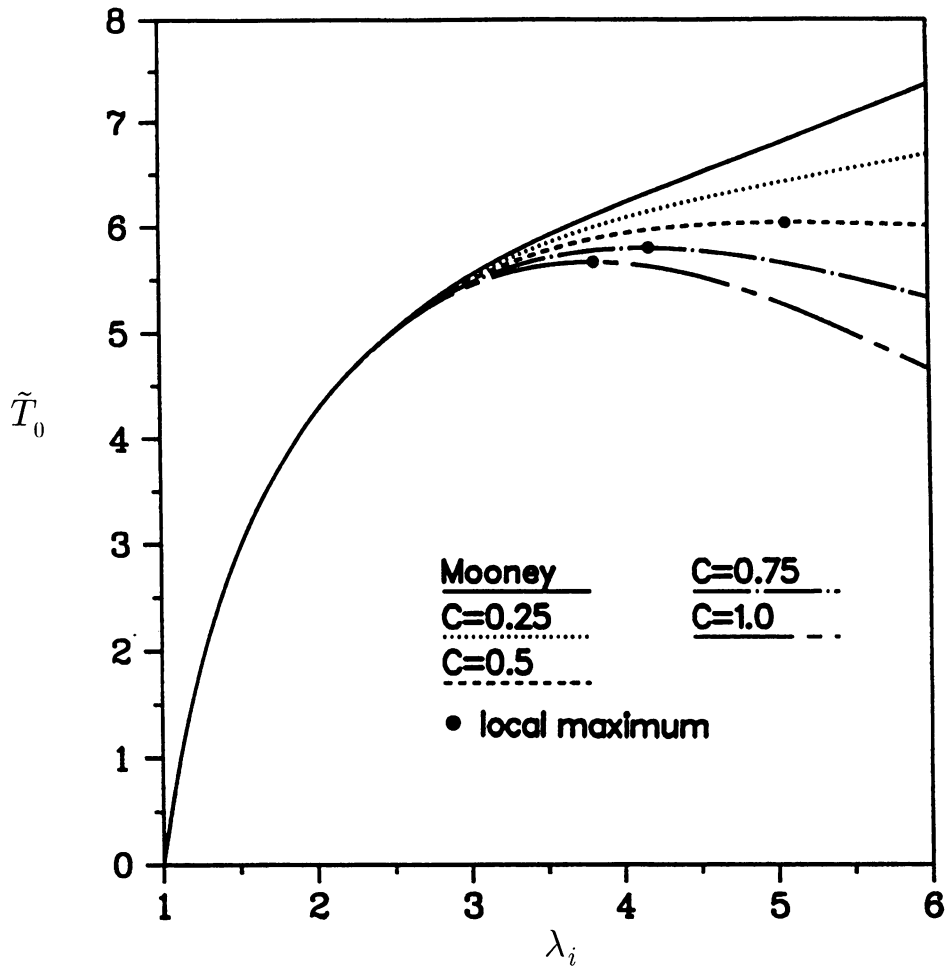

FIG. 14. External radial tensile traction vs. inner surface stretch ratio for various conversion fractions, with $\tilde{R}_o = 4.0$, $\gamma = 0.3$, $\lambda_a = 2.0$, and $\lambda_c = 6.1$

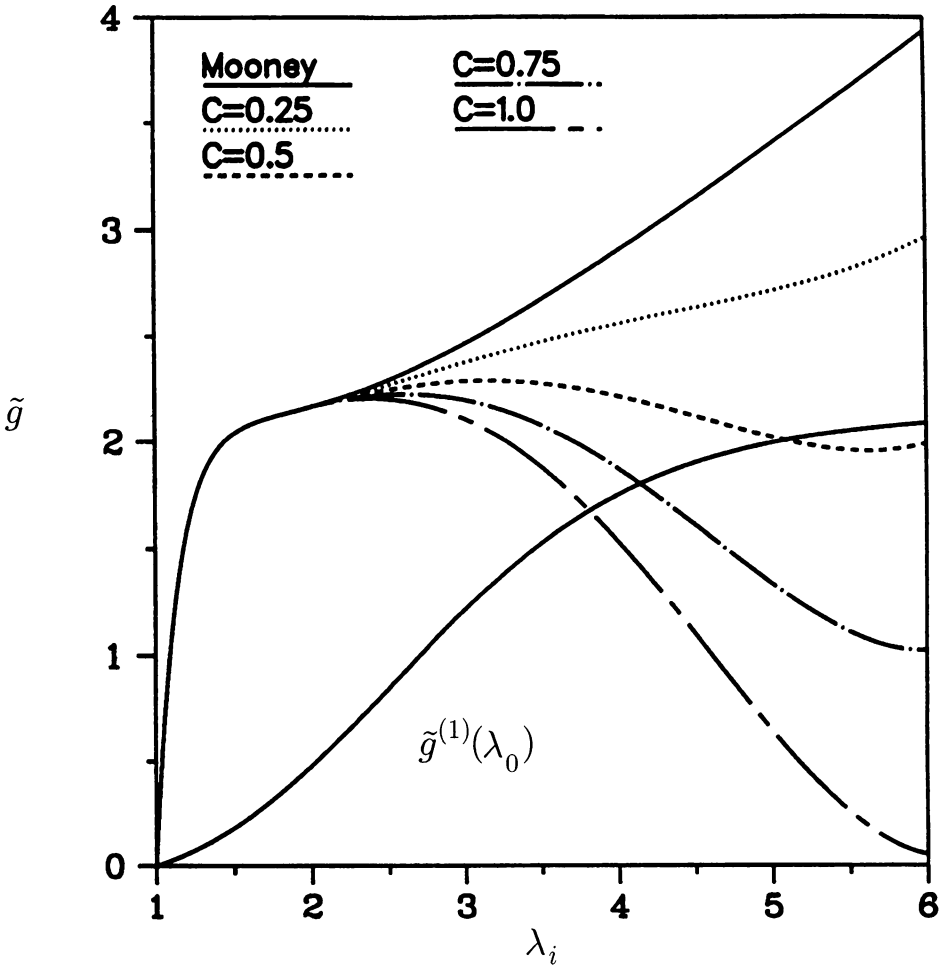

FIG. 15. g evaluated at inner and outer surfaces of sphere vs. inner stretch ratio for various conversion fractions, with $\tilde{R}_o = 4.0$, $\gamma = 0.3$, $\lambda_a = 2.0$, and $\lambda_c = 6.1$

Figure 15 shows $\tilde{g}(\lambda_i) = \widetilde{T}(\lambda_i)/\lambda_i^3$ for each of the curves of Fig. 14. The curve shown by the upper solid line in Fig. 15, representing purely elastic behavior, is denoted by $\tilde{g}^{(1)}(\lambda_i)$. Superposed is a plot of $\tilde{g}^{(1)}(\lambda_o)$ as a function of λ_i. As can be seen from the figure, $\tilde{g}^{(1)}(\lambda_i)$ and $\tilde{g}^{(1)}(\lambda_o)$ do not intersect for $\lambda_i \in [1.0, 6.0]$; this corresponds to the monotonic $\widetilde{T}_o$-λ_i relation seen for $C = 0.0$ in Fig. 14. The $\tilde{g}(\lambda_i)$-λ_i curve for $C = 0.25$ lies below $\tilde{g}^{(1)}(\lambda_i)$ for $\lambda_i \in (2.0, 6.0]$, but still exhibits the monotonic form of a "type A" material and does not intersect $\tilde{g}^{(1)}(\lambda_o)$; thus the $\widetilde{T}_o$-λ_i curve for $C = 0.25$ is monotonic. The plot of $\tilde{g}(\lambda_i)$ vs. λ_i for $C = 0.5$ shows the local maximum and local minimum of a "type C" material and intersects $\tilde{g}^{(1)}(\lambda_o)$ at $\lambda_i \approx 5.1$; the corresponding local maximum of $\tilde{T}_o(\lambda_i)$ can be seen in Fig. 14. On the interval $\lambda_i \in [1.0, 6.0]$, $\tilde{g}(\lambda_i)$ displays the single local maximum of "type B" material response when $C = 0.75$ or $C = 1.0$. The intersection points of these curves with $\tilde{g}^{(1)}(\lambda_o(\lambda_i))$ at $\lambda_i \approx 4.2$ and $\lambda_i \approx 3.8$ correspond to the local maxima in $\widetilde{T}_o$ indicated by heavy dots in Fig. 14.

It has been seen from Figs. 14 and 15 for the case of a Mooney-Rivlin material that the assumption of microstructural conversion can imply a loss of monotonicity in the $\tilde{T}_o$-λ_i relation which does not occur for the purely elastic material. Furthermore, the values of the deformation λ_i and the traction $\tilde{T}_o$ at which the local maximum occurs are lower when a greater amount of network conversion is assumed.

7. Conclusion. The qualitative properties of the T_o-λ_i relation have been investigated using the constitutive equation for continuous microstructural change presented in Sec. 2. The method of analysis of Sec. 4 shows that it is possible to use the constitutive equation to study the influence of many aspects of microstructural change, including the amount of change and the properties of the newly formed material relative to the original material. The results show that softening can significantly change the qualitative properties from those in the elastic case in which there is no microstructural change. In particular, for elastic "type A" materials, it is shown that sufficient softening can cause loss of monotonicity. For elastic "type B", the softening leads to loss of monotonicity at smaller levels of inflation and at lower loads.

References

[1] M. M. Carroll, *Controllable deformations of incompressible simple materials*, Internat. J. Engrg. **5**, 515–525 (1967)

[2] M. M. Carroll, *Pressure maximum behavior in inflation of incompressible elastic hollow spheres and cylinders*, Quart. Appl. Math. **45**, 141–154 (1987)

[3] H. E. Huntley, *Applications of a Constitutive Equation for Microstructural Change in Polymers*, Ph.D. dissertation, The University of Michigan, 1992

[4] H. E. Huntley, A. S. Wineman, and K. R. Rajagopal, *Chemorheological relaxation, residual stress, and permanent set arising in radial deformation of elastomeric hollow spheres*, Math. Mech. Solids **1**, 267–299 (1996)

[5] K. R. Rajagopal, *On Constitutive Relations and Material Modelling in Continuum Mechanics*, Report #6, Institute for Applied and Computational Mechanics, The University of Pittsburgh, 1995

[6] K. R. Rajagopal and A. S. Wineman, *A constitutive equation for nonlinear solids which undergo deformation induced microstructural changes*, Internat. J. Plast. **8**, 385–395 (1992)

[7] A. J. M. Spencer, *Continuum Mechanics*, Longman Mathematical Texts, New York, 1980

[8] A. S. Wineman and H. E. Huntley, *Numerical simulation of the effect of damage induced softening on the inflation of a circular rubber membrane*, Internat. J. Solids Structure **31**, 3295–3313 (1994)

[9] A. S. Wineman and K. R. Rajagopal, *On a Constitutive Theory for Materials Undergoing Microstructural Changes*, Arch. Mech. (Arch. Mech. Stos.) **42**, 53–75 (1991)